Journal of Hydrology: Regional Studies 50 (2023) 101532

Contents lists available at ScienceDirect

Journal of Hydrology: Regional Studies

journal homepage: www.elsevier.com/locate/ejrh

Regional evaluation of groundwater-surface water interactions using a coupled geohydrological model (SWAT+*gwflow*)

Estifanos Addisu Yimer [a,*], Ryan T. Bailey [b], Bert Van Schaeybroeck [e], Hans Van De Vyver [e], Lorenzo Villani [a,f], Jiri Nossent [a,c], Ann van Griensven [a,d]

[a] Department of Hydrology and Hydraulic Engineering, Vrije University of Brussels, 1050 Brussels, Belgium
[b] Department of Civil and Environmental Engineering, Colorado State University, Fort Collins, CO 80523, USA
[c] Flanders Hydraulics Research, Department of Mobility and Public Works, Berchemlei 115, 2140 Antwerp, Belgium
[d] Department of Water Science and Engineering, IHE Delft Institute for Water Education, 2700 Delft, the Netherlands
[e] Royal Meteorological Institute, 3 Avenue Circulaire, Brussels B-1180, Belgium
[f] Department of Agriculture, Food, Environment and Forestry (DAGRI), Università degli Studi di Firenze, Italy

ARTICLE INFO

Keywords:
Gridded climate observations
Coupled ground–surface water model
SWAT+
gwflow
Regional hydrology
Scheldt basin

ABSTRACT

Study region: The research is conducted for the Scheldt river basin, where seven major watersheds located in Belgium and partly in France are included in the analysis.
Study focus: A proper representation of groundwater–surface water interactions with (geo)hydrological models is possible via a coupled model. However, such models have disadvantages, such as complex code modifications and new tunings, and are computationally expensive. Therefore, their application on large spatial scales is limited. A newly developed model, SWAT+*gwflow* integrates the Soil Water Assessment Tool (SWAT+) with the groundwater module *gwflow* and has the potential to overcome these limitations. However, this coupled model has not yet been evaluated at a regional scale; hence, we present the evaluation of this model for regional studies using a global aquifer data over the seven watersheds in the Scheldt basin. Furthermore, we have investigated and quantified water balance components within the basin, with a focus on groundwater-surface water exchange.
New Hydrological Insights for the Region: From the results (Nash-Sutcliffe efficiency (NSE) of 0.8–0.9 for all catchments based on monthly average streamflow during calibration and validation periods), we consider the model to be a good simulator of hydrology in the basin. In addition, the simulated groundwater head shows good agreement with observed well data (with a mean absolute error of less than 0.42 m). Also, the rivers in five of the seven watersheds are found to be strongly dependent on groundwater discharge to the streams. We conclude that (1) the SWAT+*gwflow* model is capable of accurately modeling hydrological processes and state variables in the seven watersheds using global aquifer data and limited computational time, (2) the climate-gridded dataset can successfully be used for (geo)hydrological studies, and (3) the groundwater-surface water interaction increases over the years (from 1975 to 2021) with a strong increment found in the Grote Nete (3.7 fold) and upper Scheldt (2.3 fold) watersheds. These results are, moreover, promising for data-scarce regions where geohydrological modeling relies on the use of global datasets, but the mere success of this modeling application does not guarantee the accuracy of the dataset for other locations, hence, further verification is required. Furthermore, although in

* Corresponding author.
E-mail address: estifanos.addisu.yimer@vub.be (E.A. Yimer).

https://doi.org/10.1016/j.ejrh.2023.101532
Received 7 November 2022; Received in revised form 15 September 2023; Accepted 16 September 2023
Available online 20 September 2023

this study, the *gwflow* module is integrated into the SWAT+ model, it could also be integrated into other surface water models for other studies.

1. Introduction

Numerical models are widely used to represent geohydrological processes and provide insights for improved water management. These models are generally classified based on their model structure into conceptual and physically-based models, or on their level of discretization, into lumped and (semi-)distributed models (Pechlivanidis et al., 2011). There exists a vast literature that focuses on conceptual hydrological models (Choi et al., 2009; Essou et al., 2016; Raimonet et al., 2017; Vu et al., 2012; Woo and Thorne, 2006). Models have limitations as they are usually simplistic, and their underlying concepts underestimate the spatially distributed nature of hydrological processes (Martina et al., 2011; Pellicer-Martínez et al., 2015; Sreedevi et al., 2021). In Raimonet et al. (2017), conceptual models have significant pitfalls but are sometimes preferred over "complex" model setups due to reduced input requirement, relatively less uncertainty in the model parameter estimation process, and comparatively low computation time (Al-Safi et al., 2020; Blöschl and Montanari, 2010; Ibrahim et al., 2015; Nguyen et al., 2018; Sun et al., 2015). These disadvantages of both lumped and distributed models can sometimes be overcome using semi-distributed models that offer a good balance between lumped, oversimplified conceptual models and fully distributed physically based models (Pechlivanidis et al., 2011).

An additional categorization of geohydrological models can be done based on whether they simulate either surface water or groundwater using standalone "single models" or both using "coupled models" (Wang and Chen, 2021). Surface water models mostly feature a simplified representation of groundwater (e.g., Soil and Water Assessment Tool, SWAT, Variable Infiltration Capacity, VIC, ensemble of surface water hydrology study by Huang et al., 2017, etc.), while groundwater models require recharge simulated from other surface water models (e.g., Modular Finite Difference Groundwater Flow, MODFLOW) (Aliyari et al., 2019). These single models, however, are preferably coupled when groundwater-surface water interactions play a significant role in streamflow generation and general water movement in a watershed. The benefits of coupling different models are evident, especially when considering the regional scale where human and environmental processes fully interact (Barthel and Banzhaf, 2016). The surface water-groundwater (GW-SW) interactions are crucial for two main reasons: first, for watersheds where streams are supported by groundwater discharge; and second, for watersheds where water quality is governed by solute mass transport between streams and aquifers.

Different levels of integration exist when coupling models, ranging from sequential or loose coupling, in which models operate autonomously, to fully embedded or integrated models (Siad et al., 2019). Both fully and loosely coupled models have limitations that need to be considered before using them for different applications. Coupled models require higher computational time and costs. These problems are especially true for fully coupled models, which currently have been tested only in academic studies and whose potential in practical case studies is still to be demonstrated (Barthel and Banzhaf, 2016). For these reasons, loosely coupled models are considered a better alternative in practice (Wang and Chen, 2021), even if the regional geohydrological processes might be oversimplified (Barthel and Banzhaf, 2016).

Consequently, groundwater-surface water interaction has been mostly explored at a point or on a local scale, while regional scale (10^3 to 10^5 km^2) studies are rare. Since coupled models have complex computational requirements, the number of coupled model applications in regional studies is very limited (Barthel and Banzhaf, 2016). For example, Bauer et al. (2006) used a conceptual coupled model with three components (overland flow, groundwater flow, and unsaturated zone) to simulate a data-scarce area in the Okavango Delta in Botswana. One of the most common coupling combinations is the SWAT-MODFLOW coupling, dating back to 1999 (Wang and Chen, 2021). A large-scale application of SWAT-MODFLOW coupling application has been performed by Bailey et al. (2016) to model surface water – groundwater exchange in a basin in Oregon, USA. Similarly, Aliyari et al. (2019) updated the SWAT-MODFLOW codes to improve irrigation representation and tested it in a large basin in Colorado, USA. Deb et al. (2019) showed that the coupled SWAT-MODFLOW produced improved runoff simulations better than the standalone SWAT model, especially during dry periods, in two basins of Southeast Australia. A MODFLOW model was also combined with the VIC model to investigate the impacts of climate change in a basin in Northwest USA (Sridhar et al., 2018). In general, however, the major challenges from these applications are either that they are too simplified, require detailed data, or are challenging to run for fine resolution due to computational requirements.

To overcome the above-mentioned challenges, the modeling work in the present study employs the newly developed SWAT+*gwflow* model (Bailey et al., 2020) to assess streamflow and hydraulic head in seven catchments located in Belgium and partly in France. This new coupled model has the advantage of placing the physically based groundwater modeling computations, based on the physical hydrogeology and heterogeneity of the watershed system, directly into the SWAT+ modeling code (Bieger et al., 2017), and including key hydrologic features such as groundwater saturation excess flow and groundwater transfer to soils when the water table is within the soil profile. Other interactions include recharge from the soil profile to the water table, groundwater-surface water exchange through the streambed, groundwater-lake interactions, tile drainage outflow, and pumping for irrigation and municipal water supply. SWAT+*gwflow* is suitable for catchments with unconfined aquifers. The standalone SWAT+ model has a simplified representation of groundwater hydrology where linear reservoir approximations are used, leading to misrepresentation of the hydrologic processes (Deb et al., 2019; Gassman et al., 2007; Peterson and Hamlett, 1998; Spruill et al., 2000; Srivastava et al., 2006). As the aquifers in Flanders are mostly unconfined, the SWAT+*gwflow* model is an ideal hydrologic simulator. The SWAT+*gwflow* model has been successfully applied to a watershed in Georgia (327 km^2), USA, and to an intensively tile-drained watershed in Iowa (583 km^2), USA (Bailey et al., 2022).

The objective of this study is to evaluate SWAT+*gwflow* at a regional scale which has not yet been performed. The regional

application consists of seven connected watersheds. The model setup uses a global aquifer property dataset for model development. For our regional study, a gridded climate dataset for Belgium with a 5 km resolution is used, including precipitation (P), temperature (minimum/maximum/average: T_{min}, T_{max}, T_{avg}), relative humidity (RH), wind speed (W), and solar radiation (SLR). The gridded dataset was evaluated based on meteorological data from gauging stations, but the effect of using this dataset for hydrological analysis has not been explored to date. Therefore, in addition to evaluating the coupled model, this research aims to assess if the Belgian gridded data can effectively be used in hydrological modeling. Next, different water balance components are investigated and compared, focusing on groundwater-surface water interactions for the seven watersheds inside the Scheldt basin. The lack of study on groundwater-surface water interactions for the whole Scheldt basin adds novelty to our study. Finally, the use of a computationally efficient coupled model, like SWAT+*gwflow*, and a reliable gridded climate dataset are key to improving the simulation of groundwater-surface water interactions, paving the way to assess geohydrological processes at regional scales.

2. Study area and data

The study area mainly covers the northern part of Belgium, with two catchments having part of their watershed inside France (the Leie and upper Scheldt River catchments). Belgium has a mild cold season during winter (from November to March) and temperate summers (from June to September). According to the Royal Meteorological Institute of Belgium, the mean annual precipitation is around 848 mm, which shows a steady increase in annual precipitation (Brouwers et al., 2015). The topography is mainly flat, with lower elevations in the northern end and higher altitudes in the southern part of the country (Yimer et al., 2023b). The study area has very shallow groundwater, mostly in the northern part of Flanders. The northern part of Belgium (Flanders) is mostly inside the regional Scheldt River basin. The Scheldt River has a mean, maximum, and minimum streamflow of 108, 832, and 17 m^3/s, respectively. The research conducts (geo)hydrological modeling of catchments with areas varying from 510 to 5817 km^2 (Table 1).

The daily-average weather data necessary to force the model (P, T_{min}, T_{max}, RH, W, SLR) was obtained from the Royal Meteorological Institute of Belgium (RMI) for the period 1970–2021. Furthermore, the streamflow data is downloaded from Waterinfo (last accessed, 21 February 2022: https://www.waterinfo.be/). The input data for the SWAT+*gwflow* model setup are outlined in Table 1.

A common problem when applying geohydrological models is the lack of reliable, spatially and temporally extended climate data. Geohydrological models mainly require meteorological data, and as a first alternative, data from gauging stations are preferably used. In some regions, gauging stations are more sparsely distributed and scarce, hence, alternative means of obtaining meteorological forcing data are required. One alternative is to combine gauging station data with remote sensing via interpolation, producing a gridded dataset (Coustau et al., 2015; Essou et al., 2016; Funk et al., 2015; Habets et al., 2008; Jones et al., 2016; Quintana-Segui et al., 2008; Raimonet et al., 2017; You et al., 2015). For example, the Copernicus program assembles meteorological data worldwide (Cornes et al., 2018), and a similar regional effort exists, for instance, for Asia (Yatagai et al., 2009). Other widely used datasets are the Climate Hazards Group InfraRed Precipitation with Station data (CHIRPS) (Yimer et al., 2022), covering most of the world with a focus on Africa (Funk et al., 2015), and the Climate Research Unit (CRU) for the globe (Harris et al., 2020). The resolution of these gridded datasets ranges from 5 to 50 km, and they are subject to uncertainty due to the scarcity of gauging stations involved in data aggregation (Bastola and Misra, 2014; Piani et al., 2010; Tarek et al., 2021). Furthermore, the low spatial resolution, weather model bias, and inaccurate orographic specifications intensify the uncertainty in the meteorological data (Raimonet et al., 2017). Moreover, the observed solar radiation, wind speed, and relative humidity are not as commonly available as temperature and precipitation but may nevertheless be important for hydrological studies. Hence, observational gridded datasets are the major contributors to fulfilling the data demand for such variables. Therefore, we used the observational gridded dataset of RMI for forcing the geohydrological models.

3. Methodology

3.1. Background on SWAT+gwflow model

SWAT+ is a watershed model that simulates the storage and movement of water, sediment, and nutrient mass within an integrated watershed system on a daily time step. The model often is used to assess hydrological processes and water supply, subject to changes in climate and land use and land cover management scenarios. The main computational unit is the hydrologic response unit (HRU), a unique spatial unit with a combination of land use, soil, and slope classification (Arnold et al., 1998). All processes start from the HRU

Table 1
The list of model inputs required to set up the SWAT+ and the coupled SWAT+*gwflow* model.

Data	Source	Resolution
	For SWAT+ model setup	
DEM	Accessed: 1 February 2022, https://viewer.nationalmap.gov, U.S. Geological Survey, National Elevation Data	30 m
Land use	Accessed: 1 February 2022,https://remotesensing.vito.be/, VITO	10 m
Soil map	Accessed: 1 February 2022, https://www.fao.org/land-water/en/	Vector polygon
	For SWAT+*gwflow* model setup	
Aquifer thickness (cm)	Accessed: 10 March 2022, https://soilgrids.org/ (global dataset)	250 m
Permeability zones (m/day)	Accessed: 10 March 2022, https://dataverse.scholarsportal.info/dataset.xhtml?persistentId=doi:10.5683/SP2/TTJNIU (global dataset)	Vector polygon

level and are combined into landscape units (LSUs), then routed to the sub-basin level and ultimately aggregated to obtain the streamflow at the catchment outlet (Neitsch et al., 2011).

Since the groundwater component of the SWAT+ model is based on the simplified concept of a linear reservoir, the model's capability to represent groundwater hydrology is questionable. Hence, Bailey et al. (2020) developed a new physically based and distributed groundwater module for the SWAT+ modeling code. Henceforth, the coupled model is called SWAT+*gwflow*. The *gwflow* module uses a grid-based approach to solve for groundwater storage, groundwater head, and groundwater sources and sinks for individual grid cells throughout the watershed system. SWAT+*gwflow* is based on the Dupuit–Forchheimer approximation, where the vertical hydraulic gradient is assumed to be negligible, hence, the coupled model is useful for analyzing watersheds with a single-layer unconfined aquifer. The watershed is divided into a grid of cells, with each cell representing a volume (m^3) of an aquifer. For each daily time step of the SWAT+ simulation, the *gwflow* module loops through the set of grid cells, updating groundwater storage and groundwater head using a water balance equation (Eq. 1), using values from the previous day in an explicit approach. Specific groundwater sources and sinks include recharge (passed from HRUs), groundwater discharge to streams ($Q_{gw\rightarrow sw}$), stream seepage to the aquifer ($Q_{sw\rightarrow gw}$), groundwater transfer to HRU soil layers ($Q_{gw\rightarrow soil}$) for conditions where groundwater rises into the soil profile, groundwater pumping (Q_{pump}), boundary inflow/outflow (Q_{north}, Q_{south}, Q_{west}, Q_{east}), etc. The hydraulic head (h) for each grid cell is solved explicitly using Eq. (2), where Δx and Δy are the grid cell sizes, n is the time step, and S_y is the specific yield of the aquifer.

$$\frac{\Delta V}{\Delta t} = \left(Q_{rech} + Q_{sw\rightarrow gw}\right) - \left(Q_{gwet} + Q_{gw\rightarrow sw} + Q_{gw\rightarrow soil} + Q_{satex} + Q_{pump}\right) \pm Q_{north} \pm Q_{south} \pm Q_{west} \pm Q_{east} \quad (1)$$

$$h^{n+1} = h^{n} + \left[\left(Q_{rech} + Q_{sw\rightarrow gw}\right) - \left(Q_{gwet} + Q_{gw\rightarrow sw} + Q_{satex} + Q_{pump}\right) \pm Q_{north} \pm Q_{south} \pm Q_{west} \pm Q_{east}\right]\left(\frac{\Delta t}{S_y \Delta x \Delta y}\right) \quad (2)$$

To solve the water balance equations, each cell requires the following data: ground surface elevation, bedrock elevation, hydraulic conductivity (m/day), specific yield, and groundwater head (m). Cells also can be designated as "river cells" (cell intersect streams and rivers), "tile cells" (tile drain is located within the cell), and "lake cells" (cell interacts lakes). The assignment of values to cells, and the geographic intersection with HRUs, stream channels, and lakes is performed during GIS pre-processing routines, with resulting values stored in a set of input files that are read in at the beginning of a SWAT+ simulation. Complete descriptions and water balance equations are provided in Bailey et al. (2020) and Bailey et al. (2022). When in use, the *gwflow* module replaces the original SWAT+ groundwater module.

3.2. SWAT+*gwflow* model setup

The SWAT+*gwflow* model setup for individual case studies begins with catchment delineation, and then based on unique land use, soil, and slope classifications, HRUs are created. Henceforth, weather inputs are generated for the respective catchment from the observational gridded dataset. The calibration and validation periods are chosen depending on the availability of streamflow data in the catchment (Table 2). Only catchments within the Scheldt basin that are not or only mildly affected by the tidal effect are considered, as this effect is not represented in the SWAT+*gwflow* model.

The delineated catchments (see Fig. 1) have a different number of streams, sub-basins, and HRUs. Each has its defining character, where Leie and Demer feature the highest number of streams. This shows that the number of streams contributing to the main rivers, Leie and Demer, is higher than the other catchments.

Table 2
The number of sub-basins, HRUs, channels, calibration and validation periods, area, groundwater discretization, number of homogeneous hydraulic conductivity zones, and dominant zones used for calibrating the model (e.g. 10 zones are used instead of 165 zones for calibrating the upper Scheldt basin).

Catchment name	Number of sub-basins	Number of HRUs	Number of streams	Calibration period	Validation period
Kleine Nete	15	1345	99	2010–2014	2015–2021
Grote Nete	11	326	89	2000–2004	2008–2021
Dijle and Zenne	41	6086	293	2005–2009	2015–2021
Demer	37	5257	305	2005–2009	2013–2021
Dender	21	4083	243	2005–2009	2015–2021
Upper Scheldt (USC)	17	1570	197	2013–2017	2018–2021
Leie	33	2445	347	2006–2010	2016–2021

Catchment name	Area (km^2)	Grid size (m)	Number of zones	Number of major zones
Klein Nete	551.6	200	15	7
Grote Nete	509.5	200	11	5
Dijle and Zenne	2428.2	300	49	8
Demer	2204.0	200	31	6
Dender	1352.1	300	27	4
Upper Scheldt	5816.6	500	165	10
Leie	3793.7	500	107	13

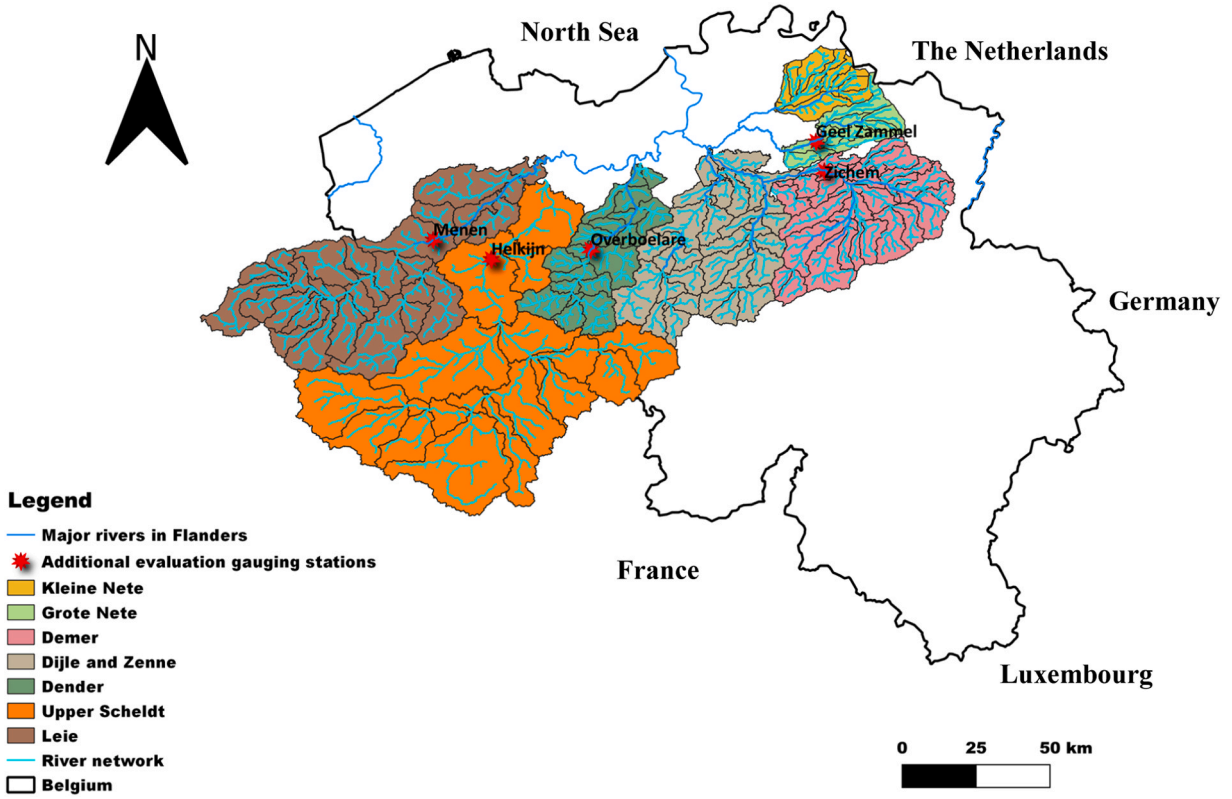

Fig. 1. The seven catchments, their boundaries, their respective river network, and validation gauging stations used for model evaluation (they are not used to calibrate the coupled model).

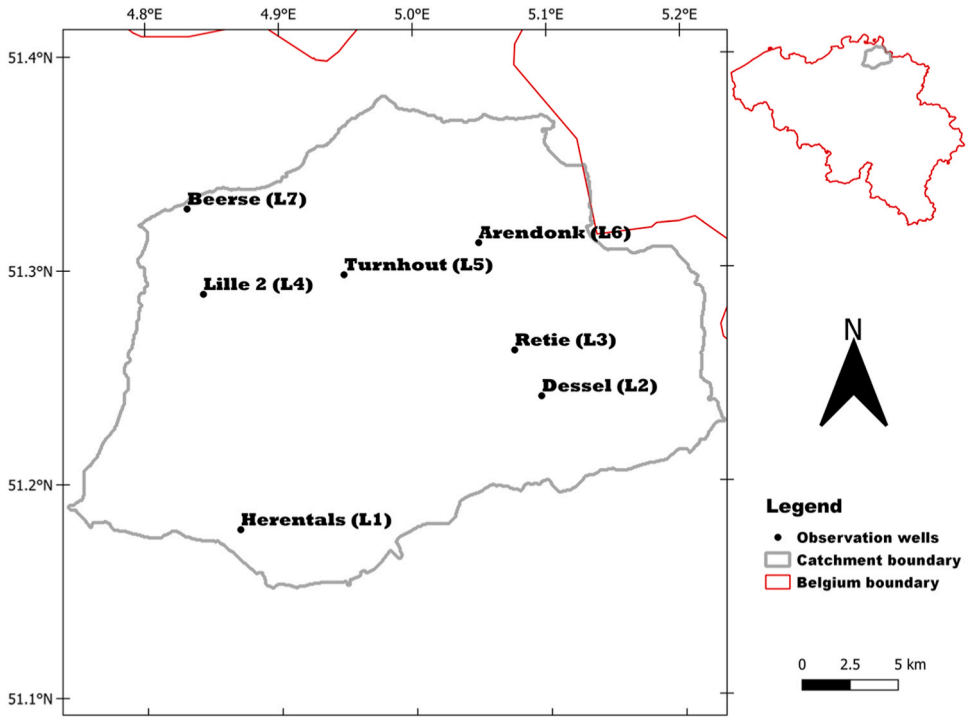

Fig. 2. The locations of observation wells inside the Kleine Nete watershed that are used for calibration and validation.

After the SWAT+ model was set up for all the catchments, the *gwflow* inputs were prepared using a Python script (the manual and the Python script can be found on the official website of the SWAT model: https://swat.tamu.edu/). This starts with discretizing the catchments into square-sized grid cells. The cell size used for each catchment is listed in Table 2. The larger a given catchment, the larger the grid size to ensure a reasonable computation time. The homogeneous hydraulic conductivity and specific yield zones are outlined based on the global database, GLobal HYdrogeology MaPS 2.0 (GLHYMPS 2.0) (Huscroft et al., 2018). Since computation time and overfitting can be an issue, limiting the number of zones for the catchment to be calibrated is vital. There are instances where the number of unique zones with different aquifer properties reaches 165 (for the Upper Scheldt catchment). Hence, we only took major zones for each catchment, as stated in Table 2. Additional input required by the groundwater module is the depth to the impermeable layer, provided by the global dataset of Shangguan et al. (2017).

After the model setup, parameters are calibrated until the statistics between measured and simulated streamflow no longer improve with continued calibration. The calibration for all the model setups constitutes the following parameter groups; hydrology.hyd (Soil evaporation compensation factor: esco, Plant uptake compensation factor: epco, Percolation coefficient: perco), river channel parameters (manning coefficient and conductivity), soil parameters (available water content: awc and soil hydraulic conductivity) and *gwflow* parameters (hydraulic conductivity, specific yield, river bed hydraulic conductivity). The final calibrated values, along with their initial and boundary values, are included in the supplementary material.

The model evaluation is done on streamflow data gauging stations different from those used for calibration. For example, for the Upper Scheldt catchment, a gauging station near Helkijn is used to evaluate the model simulation for the calibration and validation period. Similarly, for the Grote Nete catchment, a gauging station near Geel-Zammel is used. As for Dender, Leie, and Demer, streamflow at Overboelare, Menen, and Zichem is used to further investigate the optimized model parameters (see Fig. 1). The presence of water infrastructures (e.g., sluices, canals, etc.) influences the Dijle-Zenne catchment strongly (Yimer et al., 2023), hence biasing the simulated discharge (refer to supplementary material, Fig. S1). Therefore, this catchment is validated for a different time window at the catchment outlet but is not validated using other gauging stations (validation gauging stations) data. The use of streamflow at validation gauging stations to test the results obtained from the models provides a more critical assessment of the observational gridded dataset. Finally, the Kleine Nete watershed model setup is calibrated for both streamflow and groundwater head to show the capability of the coupled model to simulate groundwater head at different points in the watershed (Fig. 2). To investigate the groundwater-surface water interaction (GW-SW), the flow to and from aquifers and streams is estimated by comparing the hydraulic head and river stage. If a river stage is higher than the hydraulic head in the aquifer, water flows from the streams to the aquifers. On the other hand, if the groundwater head is higher than the stream water level, water flows from the aquifer to the rivers.

The model is calibrated using the parameter estimation tool (PEST) for mean monthly streamflow values. The model evaluation is

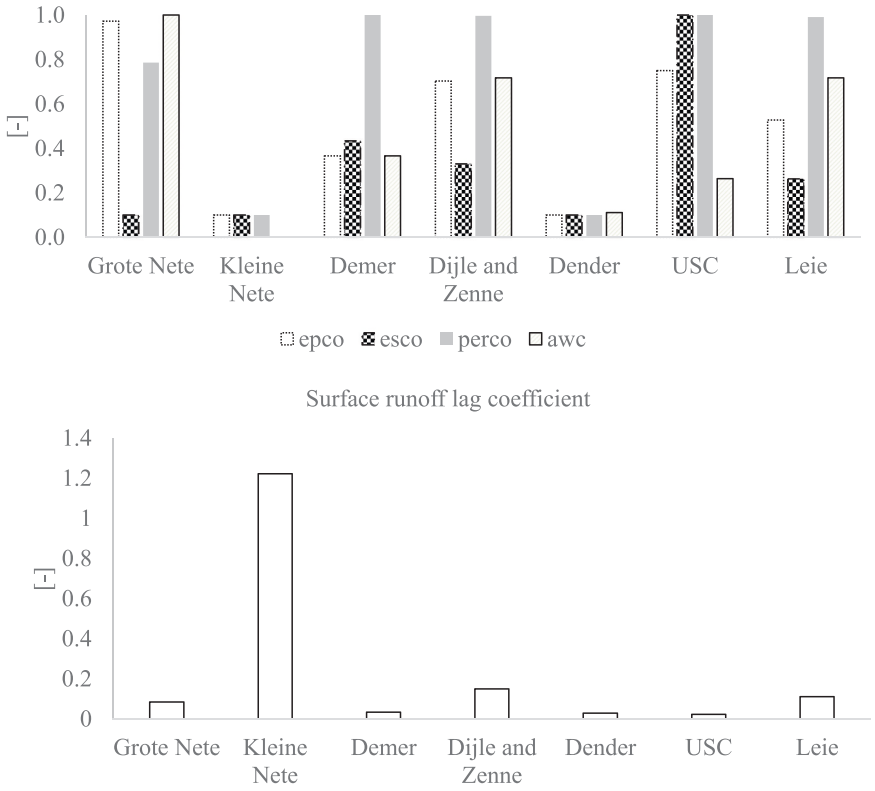

Fig. 3. The parameter that adjusts soil moisture for percolation to occur (perco), soil evaporation compensation factor (esco), plant uptake compensation factor (epco), and Soil available water capacity (awc) (top) and surface runoff lag coefficient (sur_lag) (bottom) calibrated parameters.

done using the Nash-Sutcliffe efficiency (NSE)(Nash and Sutcliffe, 1970). The classification made by Moriasi et al. (2015) is used to evaluate model simulations at monthly and daily time scales. The soil water balance at the watershed and groundwater system level (GW balance) is calculated using Eqs. (3 and 4) where P is precipitation, gwsoil is the groundwater transferred to the soil profile, Surq is surface runoff, Latq is lateral flow, Pr is percolation (equivalent to recharge), and ET is evapotranspiration; for Eq. (4), gwet is ET from

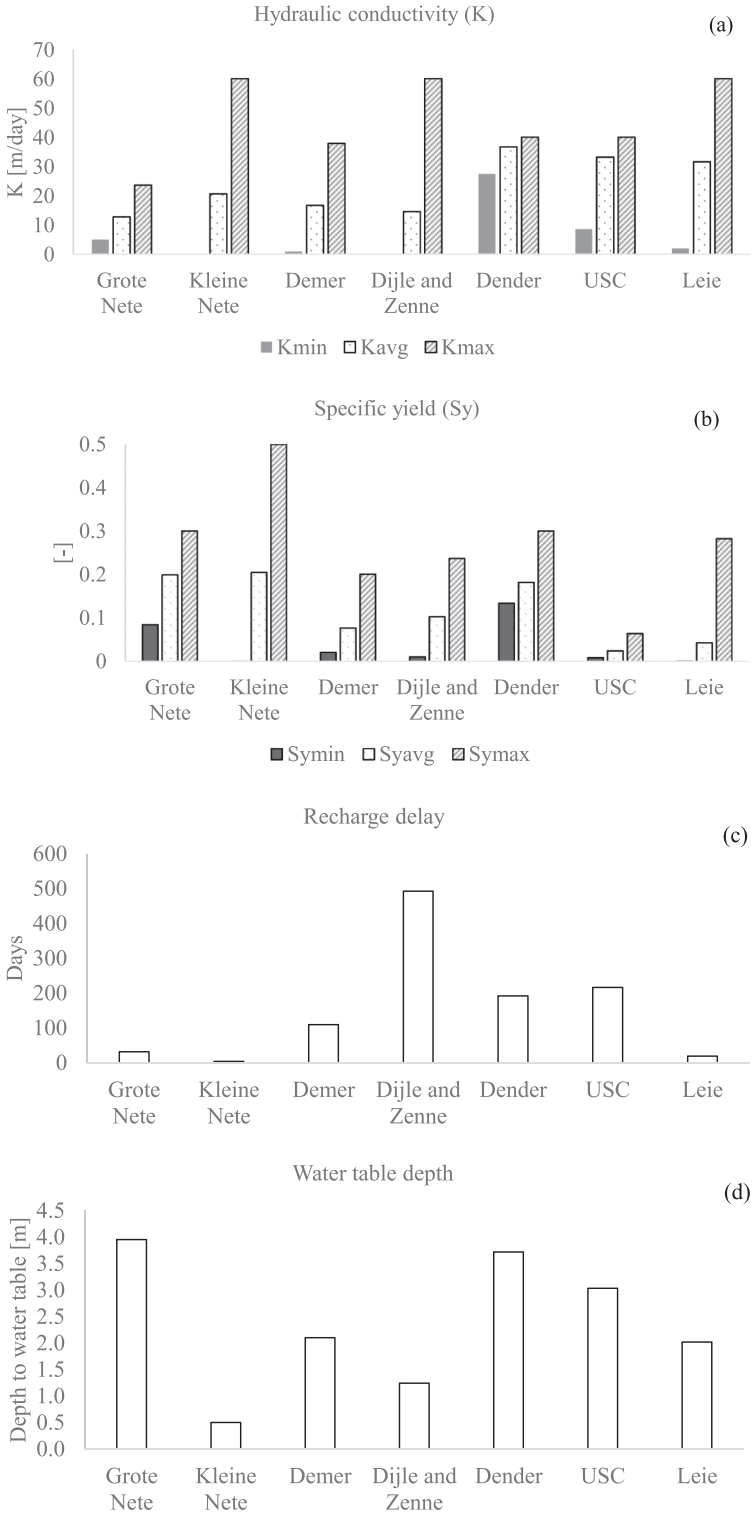

Fig. 4. The minimum, average, and maximum hydraulic conductivity (a) and specific yield (b), recharge delay (c), and water table depth (d).

groundwater, swgw is the amount of water leaving the streams to the groundwater, gwsw is discharge of groundwater to streams, satex is saturation excess flow, pump is municipal pumping, and bound is the amount of water coming from aquifers outside of the watershed, through the boundaries of the watershed.

$$\text{Water balance}_{SWAT+gwflow} = P + \text{gwsoil} - \text{Surq} - \text{Latq} - \text{Pr} - \text{ET} \quad (3)$$

$$\text{GW balance} = \text{rech} - \text{gwet} - \text{gwsw} + \text{swgw} - \text{satex} - \text{gwsoil} - \text{pump} + \text{bound} \quad (4)$$

The percentage of error at the watershed level is estimated by dividing the water balance by the total input (P + gwsoil), while for the groundwater system, the error is the difference between what is coming in and taken out of groundwater (Yimer et al., 2023a).

4. Results and discussion

4.1. Calibration and validation

The parameter that adjusts soil moisture for percolation to occur (perco) is mostly around 1.0 (Demer, Dijle and Zenne, upper Scheldt (USC) and Leie), which indicates that most of the water percolates to groundwater (Fig. 3). This mostly occurs when the soil is very permeable. A significant difference is seen mainly between Grote Nete and Kleine Nete watersheds, neighboring catchments with nearly similar characteristics (weather, soil type, land use). This can be due to the clay deposit in the Kleine Nete (Dams et al., 2009) that can hinder water movement in the soil, reducing the value of perco. The soil type in the northern part of Belgium is mostly sandy, hence, a perco value near 1.0 is reasonable. Soil available water capacity (awc) is lower wherever the water percolates towards the groundwater, leaving the soil (awc is less than perco) and vice versa. Except for the Grote Nete watershed, perco is higher than awc.

The near-one value for the Grote Nete watershed is an artifact of the calibration procedure. But, note that the awc parameter is not sensitive for this watershed, hence, the value did not affect the streamflow simulation but can affect other water balance components.

The plant uptake compensation factor (epco) shows a similar trend/values as awc except at USC and the Leie watersheds, where epco increases as awc decreases. The inverse relation between awc and epco is reasonable as whenever there is little available water, epco increases, which initiates the uptake of plant water demand from lower layers and vice versa. The soil evaporation compensation factor (esco) is mostly low, indicating that the evaporative demand is met from the lower layers of the soil.

Next, the surface runoff lag coefficient (sur_lag) is investigated, representing the fraction of water allowed to enter a stream, hence, lagging surface runoff. The lower the value of sur_lag, the more water is stored before releasing it to the nearest stream reach. The Kleine Nete catchment has a relatively higher sur_lag coefficient compared to the other six watersheds, signifying the release of water (runoff) towards the rivers more quickly than the others.

The calibrated hydraulic conductivity (K) values for the Dijle-Zenne watershed are approximately similar to the study made by Wossenyeleh et al. (2021) for the Doode Bemde wetland area inside the Dijle watershed, where the dominant aquifer is the "Brussels Sand". Similarly, the K value is similar compared to a study made by Dams et.al 2010 for the Kleine Nete catchment. According to the calibrated values, the variation of hydraulic conductivity values in the Dender watershed is low (difference between minimum (Kmin) and maximum (Kmax) hydraulic conductivity values). However, for the other watersheds, the difference between Kmin and Kmax is high (Fig. 4a). In the Dender watershed, the lowest K is more than or nearly equal to the average K value of the other basins. Therefore,

Table 3
The Nash-Sutcliffe efficiency (NSE) for the analyzed catchments for the calibration and validation periods (at daily and monthly streamflow values). This result is based on the gauging station near the catchment outlet (top) and other internal stations (bottom). The asterisk (*) indicates that validation gauging stations are unavailable or not used. Refer to Fig. 1 for the locations of the validation gauging stations.

	Nash-Sutcliffe efficiency			
	Calibration period		Validation period	
Catchment name	Monthly	Daily	Monthly	Daily
Klein Nete	0.87	0.81	0.79	0.74
Grote Nete	0.92	0.82	0.84	0.74
Dijle and Zenne	0.80	0.70	0.80	0.70
Demer	0.87	0.82	0.78	0.76
Dender	0.94	0.56	0.88	0.66
Upper Scheldt	0.86	0.83	0.89	0.84
Leie	0.94	0.87	0.93	0.88
	Based on validation gauging station			
	Calibration period		Validation period	
Catchment name	Monthly	Daily	Monthly	Daily
Klein Nete	*	*	*	*
Grote Nete	0.47	0.46	0.80	0.70
Dijle and Zenne	*	*	*	*
Demer	0.85	0.80	0.86	0.80
Dender	0.70	0.54	0.89	0.75
Upper Scheldt	0.70	0.63	0.80	0.56
Leie	0.94	0.82	0.91	0.84

the relatively high K values are because of the very conductive nature of the aquifer material.

The Dender catchment's minimum Sy values (after calibration) are higher or approximately similar to the rest of the catchments average Sy values. The higher the Sy values, the higher the proportion of groundwater volume removed for a given change in

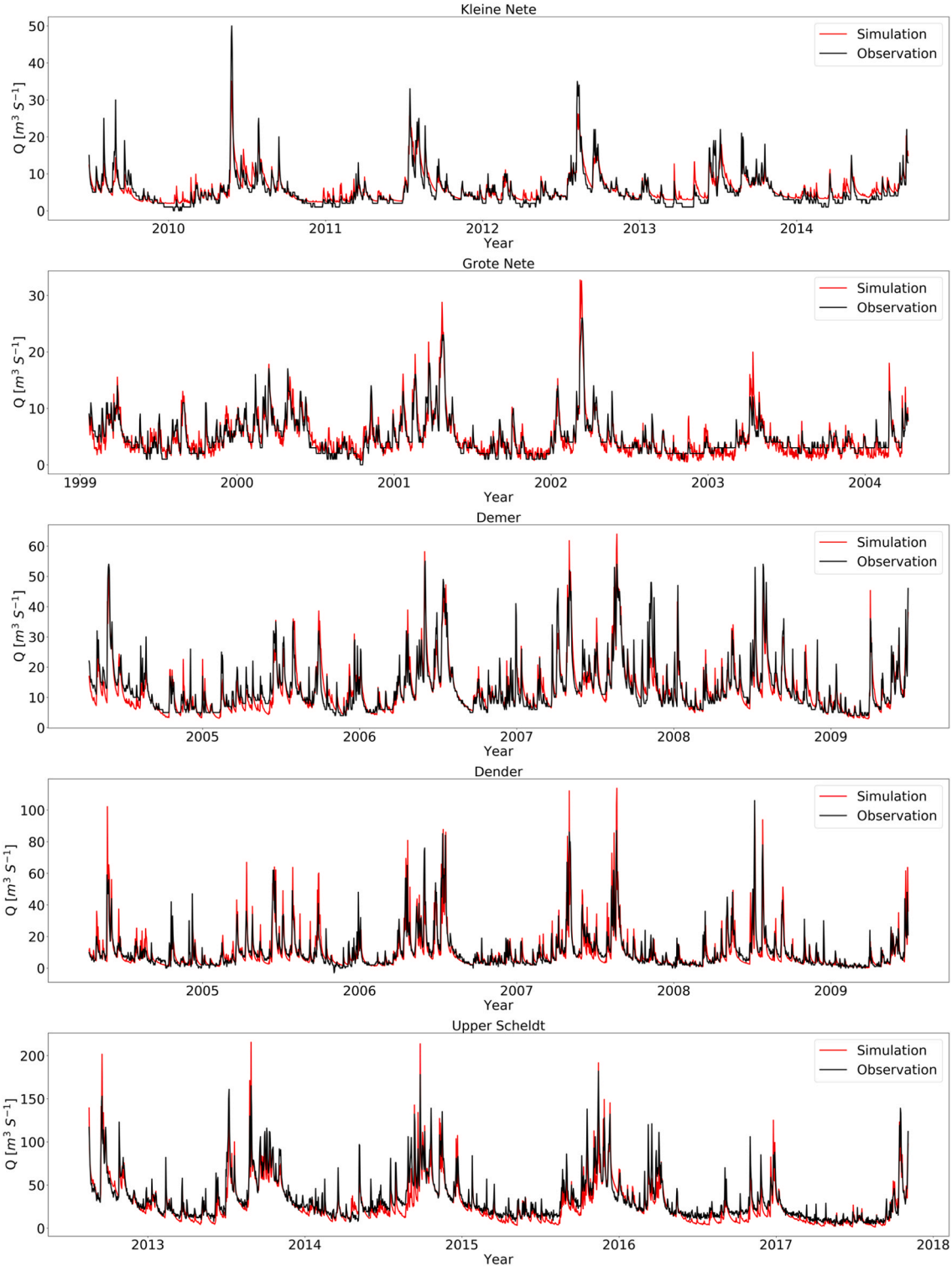

Fig. 5. Comparison between streamflow model output and measured values for calibration and validation periods for the Kleine Nete, Grote Nete, Demer, Dender, and upper Scheldt catchments.

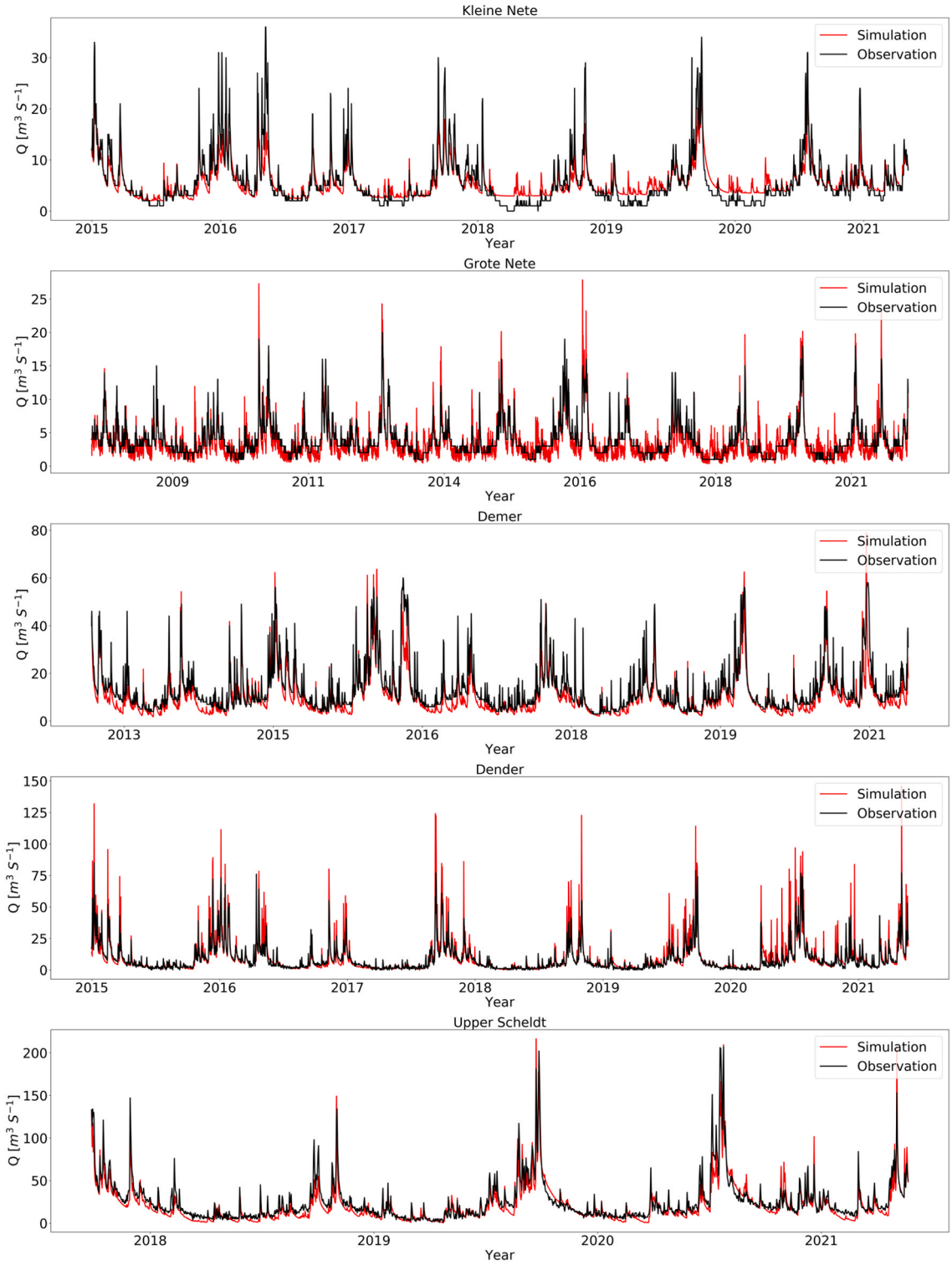

Fig. 5. (*continued*).

groundwater head. When it comes to the number of days it takes for water to reach the water table, the Dijle-Zenne watershed requires, on average, the most extended number of days to recharge the aquifer (493 days), which can be attributed to the mass extent of urbanization (e.g., Brussel, Leuven, Mechelen, etc.). Impermeable surfaces (e.g., pavements in urban areas) lead to more surface runoff, hence, less groundwater recharge (Foster et al., 1994; Minnig et al., 2018; Tam and Nga, 2018). On the other hand, the Grote

Nete, Kleine Nete, and Leie have the shortest recharge delay (ranging between 4 and 31 days). We refer to the supplementary material for the full list of parameters used for each model and their final calibrated values.

Table 3 shows the NSE values for all calibration and validation periods for monthly and daily streamflow values. All values range between 0.6 and 0.8, and according to Moriasi et al. (2015), the models have satisfactory to very good results. The analysis for the daily streamflow indicates successful modeling of the high and low flows (refer to the supplementary material (Fig. S2) for flow duration curves), signifying the appropriateness of the model and the data used to set up the model (Fig. 5). Here, a well-performing model is one of the indications of accurate weather inputs; hence, the gridded dataset is instrumental. Moreover, the model simulations at gauging stations different from those used for calibration were also checked, and the results indicated good similarity between measured and simulated streamflow (NSE above 0.46).

As shown in Fig. 5, there is a bit of noise in representing the baseflow for the Grote Nete watershed, mainly during the validation period, a slight overestimation of baseflow for the Kleine Nete and a small underestimation for the Demer catchments by the model is seen. In the rest of the cases, the baseflow is well simulated. Baseflow is a dominant feature in the rivers across Flanders (Van Camp et al., 2010), so capturing baseflow by our model is vital.

4.2. Water balance

The water balance closure is an essential criterion for assessing the quality of the model simulations. The soil water balance here closes for all the models with less than 0.4% based on the analysis at the watershed level. The groundwater error is very low (compared to a study made by Bailey et al., 2020), with a maximum difference of 5.8 mm for the Dijle and Zenne catchment (Table 4). The reason for such discrepancy can be uncertainty on inter-aquifer boundary inflow, model parameter estimation, inputs, numerical solver, rounding off, the exclusion of pumping, etc. The ability of the model to reasonably close the soil water balance and capture the streamflow makes the model setup useful for understanding basin average water balance components and long-term streamflow conditions. However, to fully capture the geohydrology in the Scheldt basin, other aspects, such as simulated soil moisture, deep percolation, and other water balance components, need to be verified. In addition, assessing water balance at groundwater and watershed levels strengthens the evaluation of the coupled model.

The basin average water balance components indicated that the average precipitation ranges between 773 and 844 mm across the seven watersheds with an average of 810 mm. Part of this goes to surface runoff (ranging between 124 and 225 mm), evapotranspiration (519–695 mm), and lateral flow, which accounts for a small portion of the total water budget (ranging between 0.01 and 5.6 mm). Saturated excess flow is also dominant in all the watersheds, with an average value of 90 mm (Fig. 6).

The ET is highest in the Dijle-Zenne and lowest in the Dender watersheds but maintains nearly similar values in the rest of the watersheds, hence, ET does not vary significantly across the different watersheds. The difference in ET between the Dijle-Zenne and Dender can be due to the difference in the land use type, where urban areas and forests are more dominant in the Dijle-Zenne than in the Dender (Fig. 7). Agricultural/forestry in the Dijle-Zenne and Dender accounts for 66% and 40.7% of the total area, respectively, hence, the ET is expected to be higher for the Dijle-Zenne than the Dender watershed. The basin average surface runoff also does not vary considerably across the catchments, but the highest runoffs are observed in the Dender, Grote Nete, and Kleine Nete. As for the saturated excess flow, when groundwater is above the ground surface, it is routed to the nearest stream, which is prevalent in the Kleine Nete and Grote Nete watersheds, which can be due to the shallow nature of groundwater in those catchments.

The groundwater flow into the system from the adjacent catchment is found to be dominant for the Kleine Nete, Leie, and Dijle-Zenne watersheds (Fig. 8). The aquifer in the Dender catchment receives only a small portion of groundwater from adjoining watersheds. The neighboring watersheds, Grote Nete and Demer have nearly similar boundary inflows into their aquifer and yearly variations. In most of the catchments, it is seen that there are annual variations that indicate the dependence of boundary flow in the groundwater flow/hydraulic head variability from the feeding aquifer. Since the amount of boundary flow is significant, any form of eco-geohydrological impact on one watershed (e.g., pumping, drought, deforestation, etc.) can affect others within the Scheldt basin. Note that calibrating the model for both streamflow and groundwater head can result in groundwater head values being different from those attained while calibrating the model for only streamflow, affecting boundary flow and, in general, the groundwater fluxes. Note that the model setup is only validated for streamflow, hence, to ensure appropriate water balance components are attained, a multi-variable model verification/calibration protocol is needed. Also, the *gwflow* module should allow users to specify a mix of boundary conditions (currently supports either constant head or no flow boundary), which can ultimately affect boundary flux and other water

Table 4
The watershed soil water balance difference between input and output (error and error as % of the input) and groundwater balance error (mm).

	Watershed soil water balance				Groundwater balance error	
Catchment name	Calibration		Validation		Calibration	Validation
Klein Nete	-0.17%	1.57 mm	0.00%	-2.15 mm	-0.13	-0.30
Grote Nete	0.30%	3.26 mm	0.15%	1.41 mm	-0.43	-0.16
Dijle and Zenne	0.33%	3.40 mm	0.36%	3.60 mm	5.31	5.78
Demer	0.09%	2.97 mm	-0.04%	-1.23 mm	0.79	-0.09
Dender	0.11%	1.04 mm	0.10%	0.85 mm	0.44	-1.27
Upper Scheldt	-0.49%	-5.59 mm	0.39%	3.91 mm	-0.82	0.77
Leie	0.23%	-3.24 mm	0.29%	3.69 mm	0.21	0.23

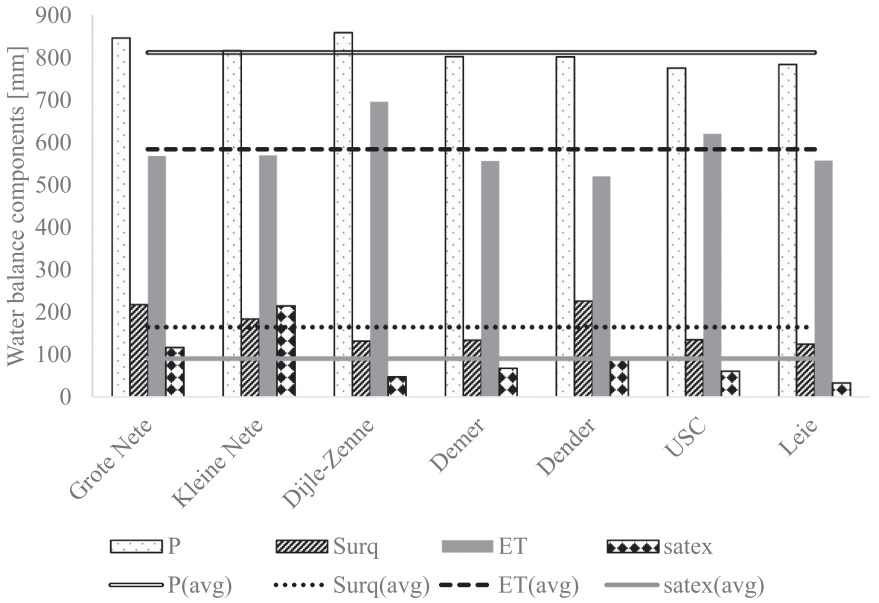

Fig. 6. The basin average water balance components, precipitation (P), surface runoff (Surq), evapotranspiration (ET), saturated excess flow (satex), and the average of the seven watersheds (in mm).

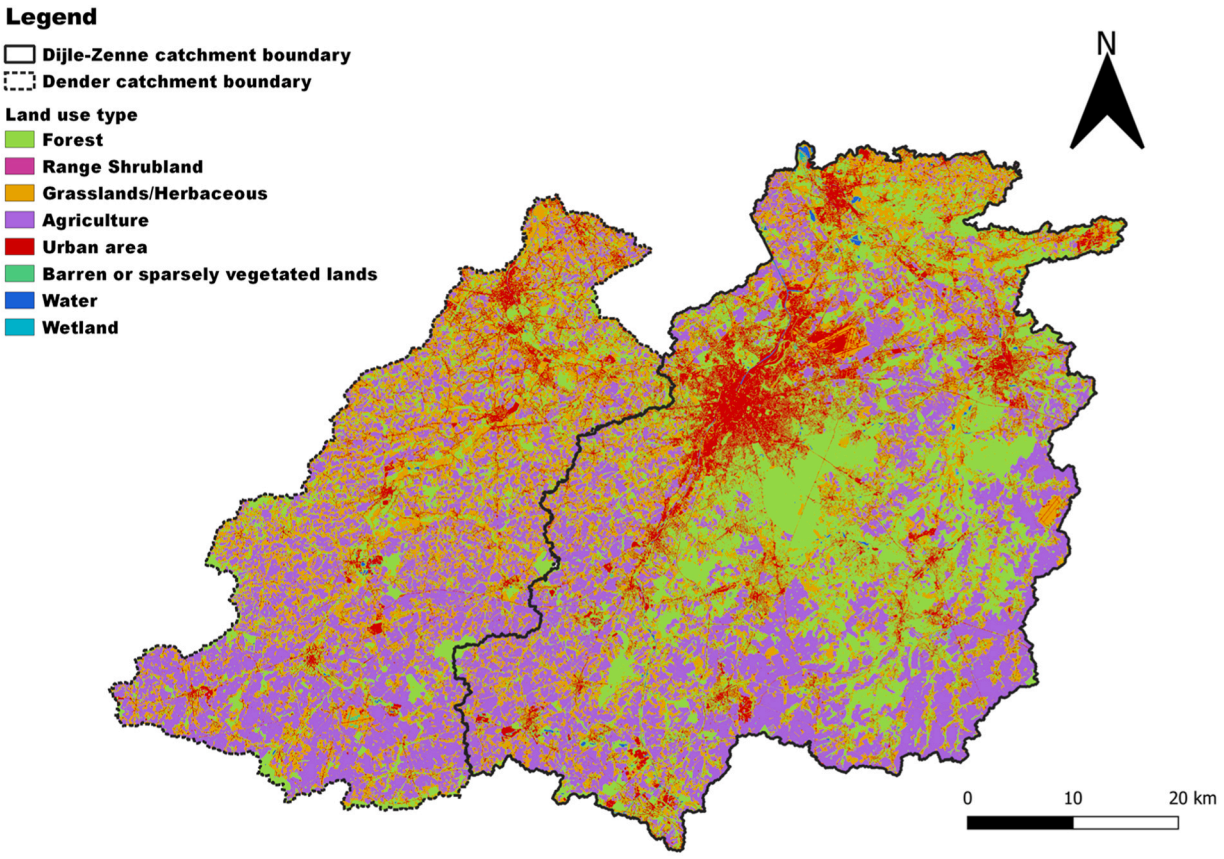

Fig. 7. The land use type difference in the Dijle-Zenne and Dender watersheds.

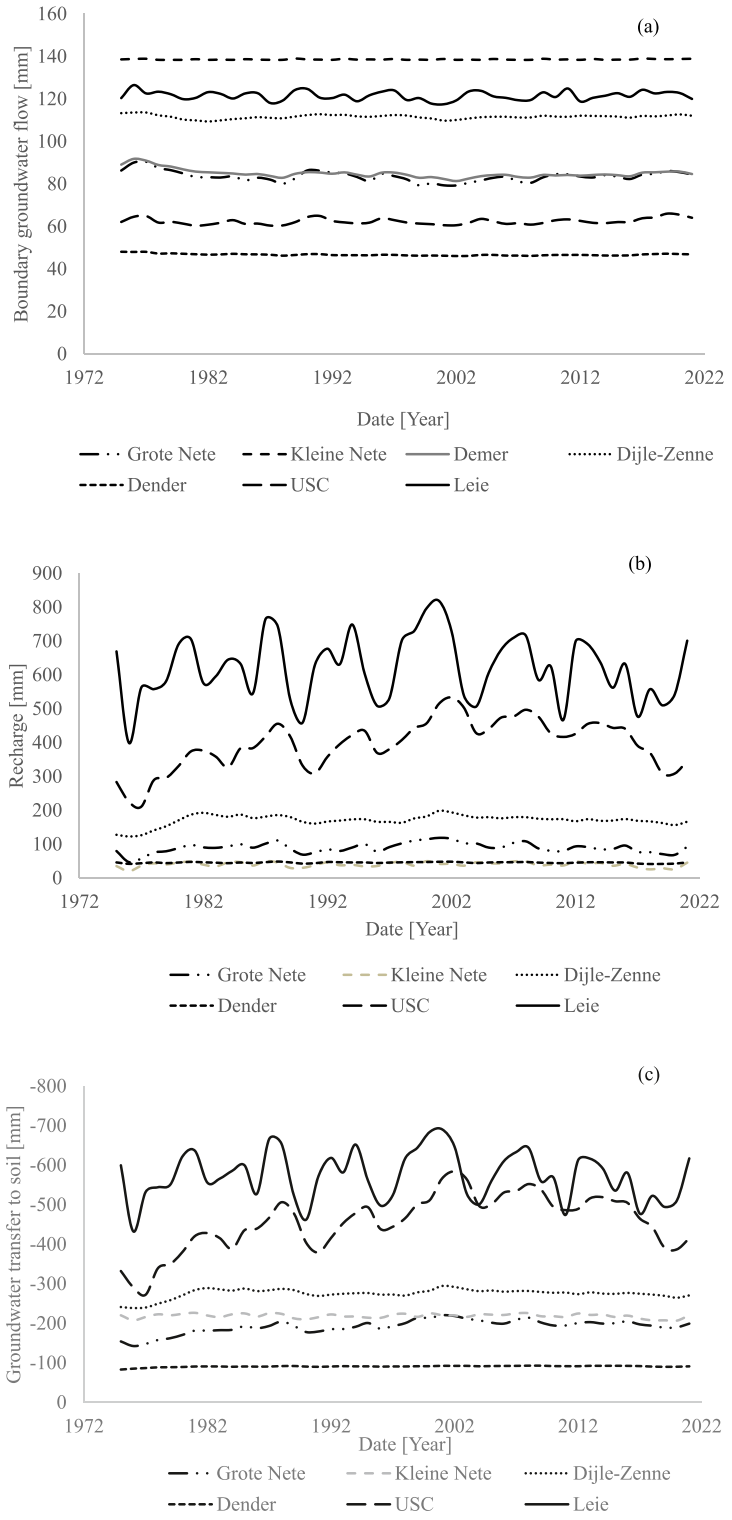

Fig. 8. The boundary groundwater flow at catchment boundary (a) and recharge (b) and groundwater transferred to the soil profile (c) given in mms.

balance components.

Recharge shows considerable temporal and spatial variations among the seven watersheds. The highest recharge value is seen in the Demer watershed, but since it is high compared to other watersheds (average value of 3172 mm), we exclude it from the plot as it

distorts the view for the other catchments. The Demer watershed needs to be calibrated for multiple aspects (e.g., groundwater head, soil moisture), which can ultimately lead to plausible recharge values. However, it is important to note that the water that reaches the water table can also be taken back by the groundwater soil interaction (gwsoil), hence, the net recharge is the difference between recharge and gwsoil. Recharge and gwsoil show a similar trend; if one increases, the other decreases, and vice versa. This is plausible as the rise of the groundwater table due to recharge leads to groundwater transfer to the soil profile if the aquifer is too shallow.

GW-SW interaction has a higher magnitude for the Grote Nete, Kleine Nete, Demer, USC, and the Leie, while it's insignificant for the Dijle-Zenne and Dender watersheds. The groundwater discharge into those rivers is low, which can be due to the lower conductivity of

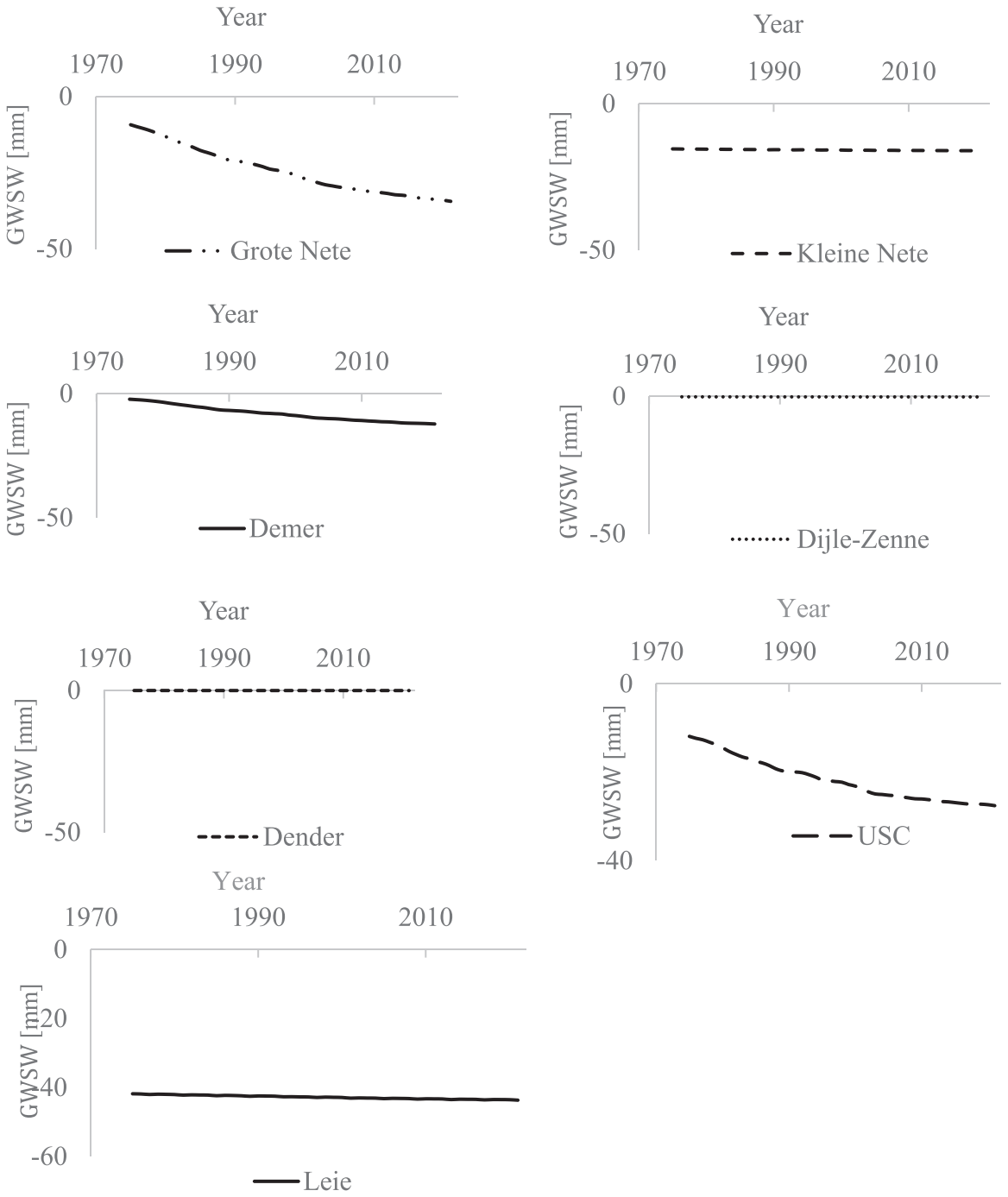

Fig. 9. Groundwater-surface water interaction (GWSW) in the seven watersheds from 1975 to 2021. The values are negative as they are sinks (taken out of the groundwater) and given in mm's.

the streambed, blocking water inflow to the streams. The interaction is seen to increase over time for all the watersheds, indicating the increasing influence of the groundwater system in feeding the streams in the Scheldt river basin (Fig. 9). This trend can be because of the decreasing streamflow due to climate change, hence, increasing groundwater discharge to the rivers.

The GW-SW interaction plays a vital role during extremely low streamflow moments (e.g., during drought), which leads to rivers

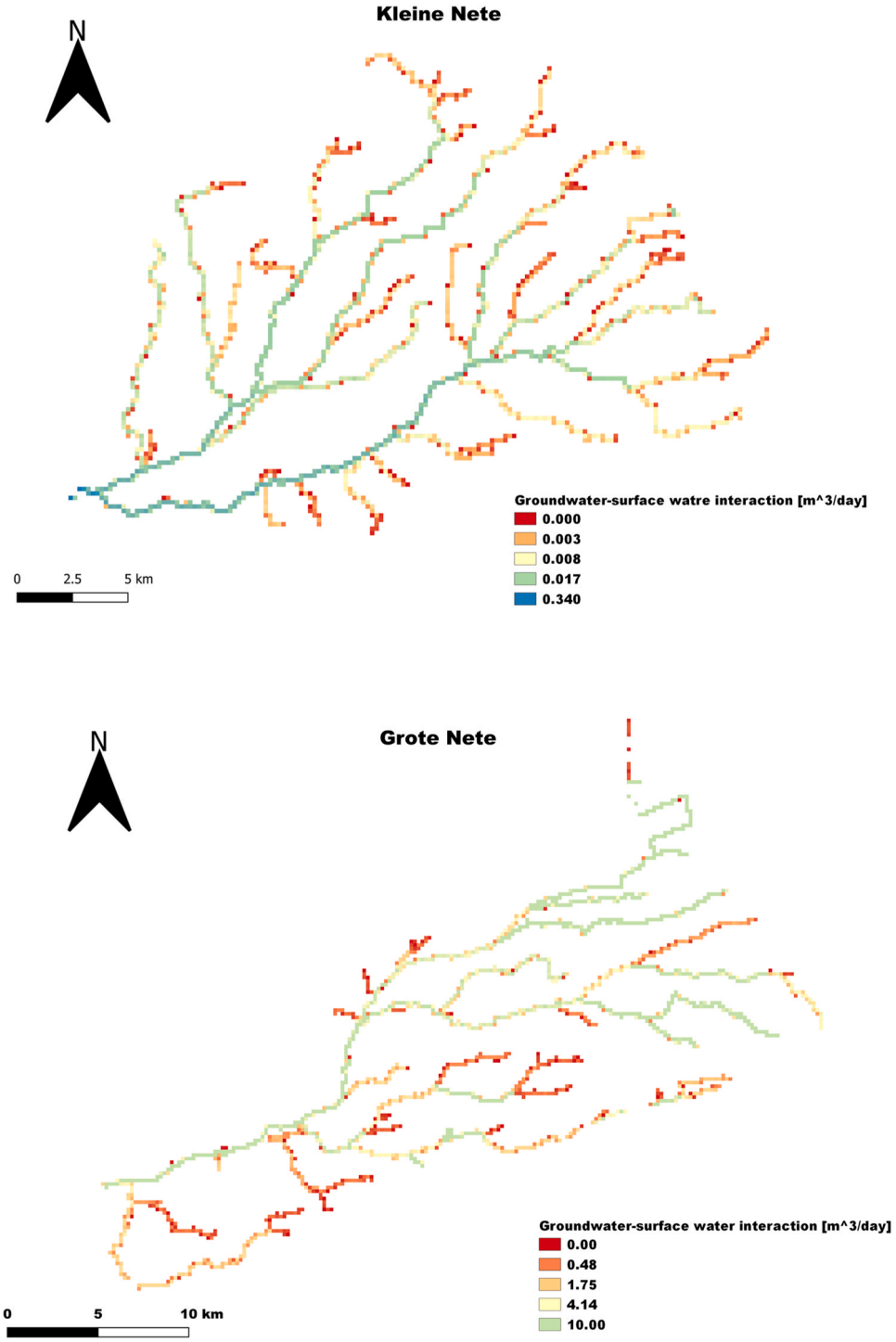

Fig. 10. Groundwater-surface water interaction in the seven watersheds during summer time (1st August 2007). The numbers stand for minimum, quartiles (three or four quartiles), and maximum values of GW-SW interactions. As for the Leie, the third quartile and maximum values are the same. As indicated in the previous figure, the USC and Leie watersheds constitute significant baseflow.

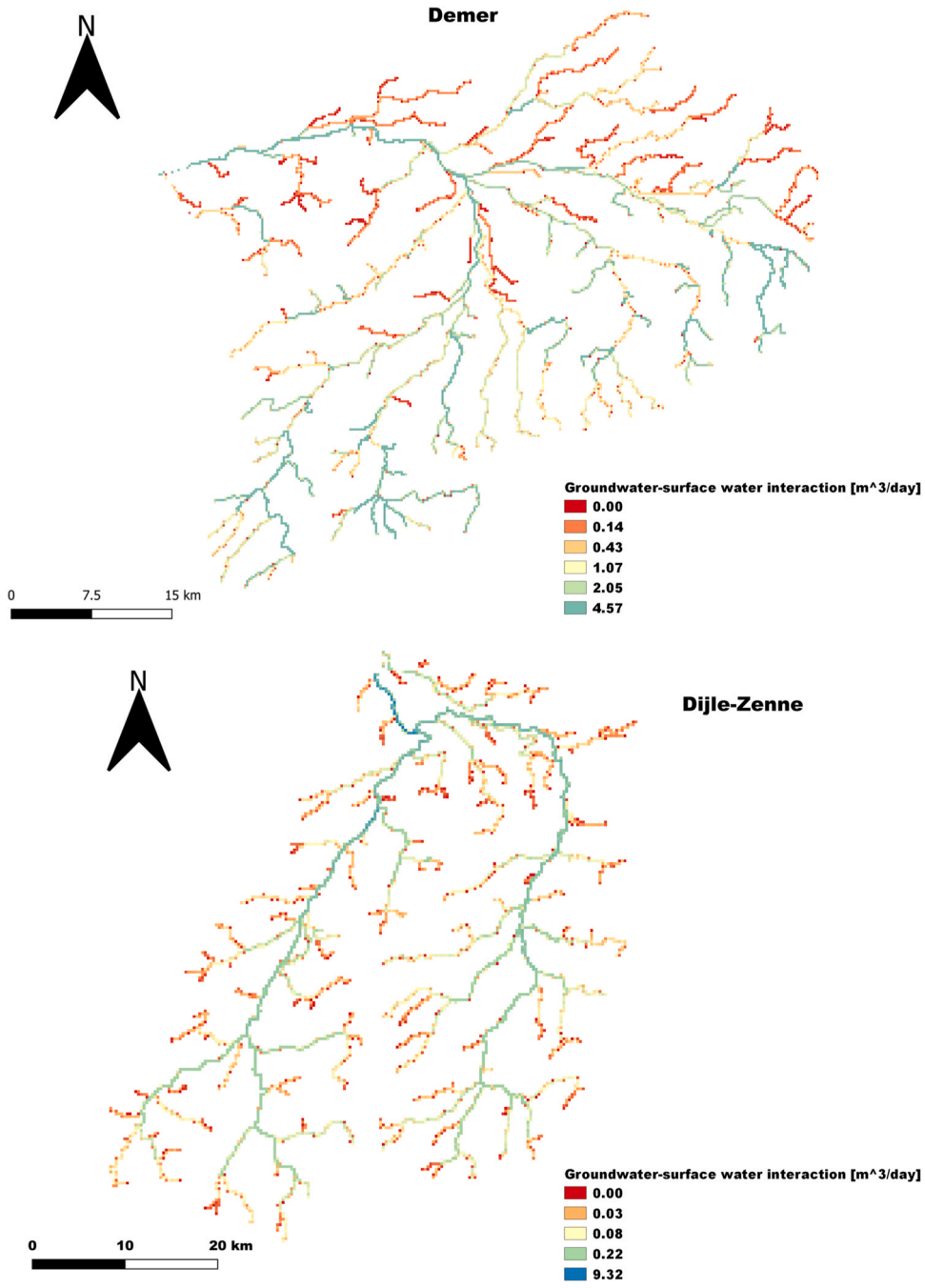

Fig. 10. (*continued*).

being fed with groundwater discharge (Fig. 10). This is the reason for selecting a day during the summer month to show GW-SW interaction in Fig. 10. Note that GW-SW interaction and saturated excess flow form the total baseflow. As seen in Fig. 10, major interaction is seen on the main river reaches of the watersheds as compared to the tributaries. Also, the USC and Leie are shown to be dominated by a large flux of groundwater into their respective rivers. On this specific date (during summer), the flow in all seven watersheds is from groundwater to the streams. The reason is because of groundwater influence (shallow water table), hence, baseflow dominates.

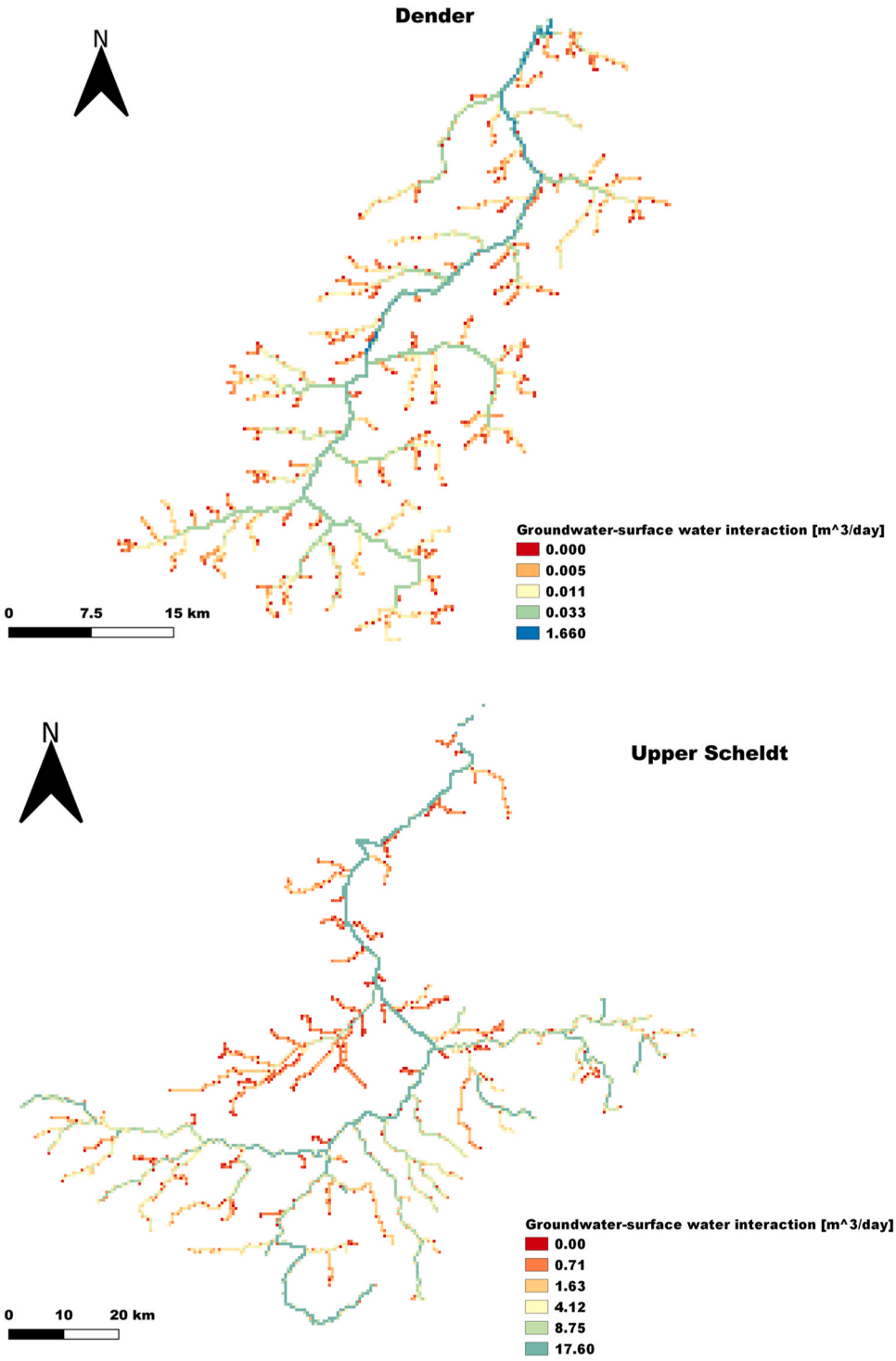

Fig. 10. (*continued*).

4.3. Groundwater output

The results presented above for the Kleine Nete watershed used model runs calibrated using only streamflow data. For the second setup, we performed a calibration that included groundwater head and streamflow as calibration targets. The results suggest that the model can capture the hydraulic head and streamflow simultaneously (Tables 3 and 5). For example, the groundwater head at Beerse,

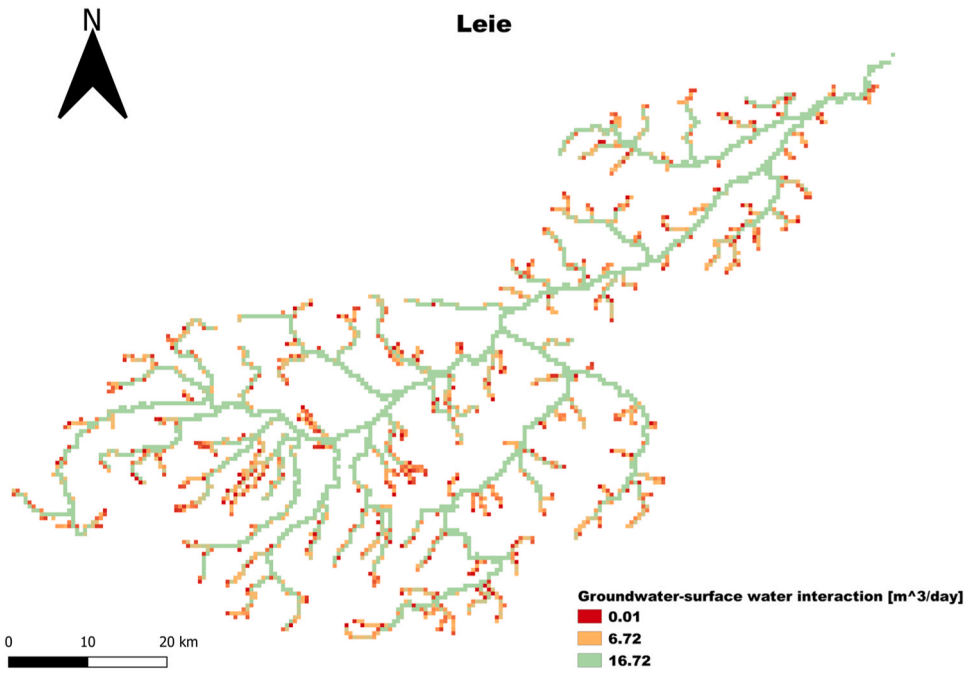

Fig. 10. (*continued*).

Table 5
The root mean square error (RMSE) and mean absolute error (MAE) for all well locations (See Fig. 2 for L1, L2, L3, etc.) during calibration and validation periods.

Period	Indices	L1	L2	L3	L4	L5	L6	L7
Calibration	RMSE	0.14	0.36	0.45	0.42	0.26	0.25	0.4
	MAE	0.11	0.3	0.37	0.34	0.22	0.21	0.31
Validation	RMSE	0.42	0.4	0.51	0.5	0.29	0.4	0.44
	MAE	0.34	0.34	0.42	0.39	0.24	0.32	0.35

the seasonality, and the groundwater head values are simulated very well (Fig. 11). In general, the groundwater head in the other wells was also captured reasonably with a mean absolute error (MAE) less than 0.42 m (Table 5). This result is better than what is achieved by Bailey et al. (2022), Aliyari et al. (2019), and Guevara Ochoa et al., (2020).

The major advantage of the coupled model is that recharge from the surface processes is automatically estimated and transferred to the groundwater grids to simulate groundwater processes. Moreover, the spatial variability of different fluxes (e.g., recharge) can outline locations with high and low values, as shown in Fig. 12 for exemplary large watersheds, upper Scheldt, and the Leie. The recharge values shown (USC: around 0.3 mm/day * 365 =109.5 mm/year and for Leie: around 0.8 mm/day * 365 = 292 mm/year) in Fig. 12 are plausible as it gives nearly similar recharge values as estimated by Zomlot et al. (2015) and Van Camp et al. (2010).

4.4. Discussion

The SWAT+*gwflow* coupled model produced results within reasonable computation time, where running the models took minutes on a personal computer. The only issue working with this model is the extended time needed to calibrate the model with PEST, which is attributed mainly to the existence of different hydraulic conductivity zones that make the number of parameters to be calibrated high. However, due to our approach of reducing the number of zones based on areal coverage (small zones are removed from the calibration), the calibration time has decreased. Small-scale applications of coupled models (Galbiati et al., 2006; Guzman et al., 2015; Kim et al., 2008; Luo and Sophocleous, 2011; Menking et al., 2003; Sophocleous et al., 1999) neglect basin-wide interactions, hence, the regional application as done on the Scheldt basin by accounting this interaction helps to simulate and understand the regional scale geohydrology.

The model parameters have physical meaning, hence, it was easy to fix their minimum and maximum value and assess the final calibrated parameter values. For example, the hydraulic conductivity and specific yield are within the range suggested in Dams et al. (2009) for the Kleine Nete watershed. The calibrated model parameter values for the Dijle-Zenne watershed are similar to those obtained by Wossenyeleh et al. (2021). The parameters can indicate the geohydrological variability among the seven watersheds which is shown with distinct surface and groundwater-related parameters.

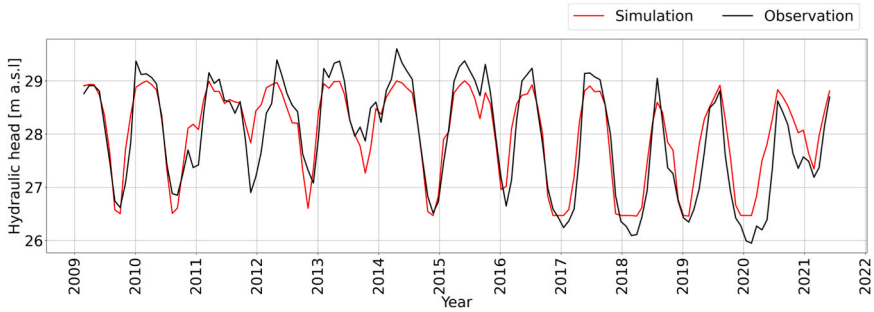

Fig. 11. The result of simulated groundwater head values during calibration (2010 – 2014) and validation (2015 – 2021) periods for the well at Beerse (in Fig. 2, the location of the well can be seen).

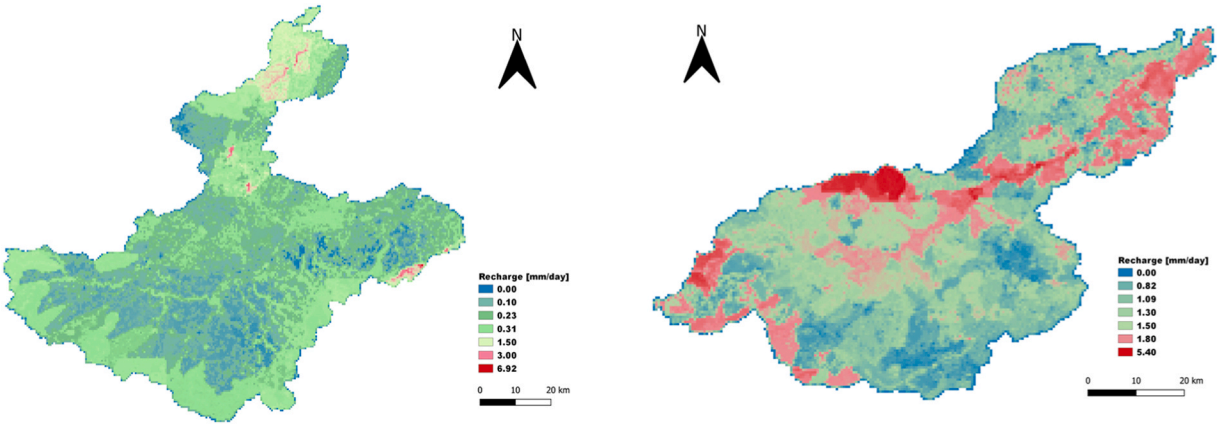

Fig. 12. The spatial variability of recharge for the upper Scheldt (left) and the Leie watersheds (right) during the dry summer of 2019.

Using the coupled model, we can better understand hydrologic fluxes, particularly GW-SW interaction, in the study basin. Since such interactions have not been measured in the field, this study needs to be verified using measurement data. There are several methods to measure such interactions, for example, using tracer test (Harvey and Bencala, 1993), permeameter, and seepage meter (Avery, 1994), based on streambed temperature (Conant Jr, 2004; Devito et al., 1996; Fryar et al., 2000; Keery et al., 2007; Silliman and Booth, 1993), electrical resistivity (Nyquist et al., 2008) and measuring streamflow at baseflow condition. The increasing trend in the amount of water being discharged from the aquifer into the rivers inside the Scheldt basin indicates the need to assess this interaction which can affect water quality (Lamontagne et al., 2005), wetland processes (Jolly et al., 2008) and in general the ecological function of the various water systems (Hayashi and Rosenberry, 2001; Ludwig et al., 2005; Van der Kamp and Hayashi, 2009).

The study made by Zomlot et al. (2015) for the whole of Flanders using the surface water model WetSpass indicated the prevalence of baseflow across the rivers. This is also confirmed in the study of Van Camp et al. (2010) using the MODFLOW model, where they estimated the baseflow to vary between 69% and 87% of streamflow. Therefore, baseflow is a crucial component to investigate inside the Scheldt basin closely, and from the streamflow simulation, it is seen that our model captures the baseflow. The variation of GW-SW interaction (which shows an increasing trend in the Scheldt basin) is vital to assess its impact on water quality and the ecological functioning of the rivers. The model setup we developed can also help to investigate how GW-SW interaction will evolve in a changing climate, as done by Waibel et al. (2013), which will be helpful for policymakers to act on the impact accordingly.

In addition, the annual average recharge estimated by the SWAT+*gwflow* model setup indicated approximately similar values as estimated by Zomlot et al. (2015) and Van Camp et al. (2010) for most of the watersheds. An additional groundwater model output is boundary inflow that shows the interaction with adjoining watersheds. This model output is essential as the impact on one watershed can affect the water-receiving aquifer, hence, integrated water resource management at a basin level is required, and this inter-basin interaction can be obtained from the coupled model (SWAT+*gwflow*). It is vital to calibrate the regional scale model for streamflow and groundwater head, as done for the Kleine Nete watershed, to capture the water balance components more accurately.

5. Conclusion

Large-scale studies using coupled groundwater-surface water models are rare due to complex coupling and computation issues. In this work, we evaluated a distributed (geo)hydrological model at a regional scale using global aquifer datasets and a gridded

meteorological observational dataset of Belgium within seven watersheds inside the Scheldt basin (France and Belgium). We focused on groundwater-surface water interactions in the basin, as these have yet to be studied in the Scheldt basin spatially and temporally.

The streamflow in all the catchments was simulated very well, with NSE values above 0.6 for both calibration and validation using daily and monthly streamflow values. In addition, the model output evaluation is performed using additional independent gauging stations (validation gauging stations). The result suggests a good agreement between measured and modeled streamflow with NSE values above 0.46, signifying that the SWAT+*gwflow* model represents well streamflow in a large part of the Scheldt basin. Moreover, the gridded dataset gave satisfactory results while forcing the (geo)hydrological model, implying its usefulness for such regional studies. Next, the groundwater-surface water interaction is found to be increasing over the years (from 1975 to 2021), with a strong increment found in the Grote Nete (3.7 fold) and upper Scheldt (2.3 fold) watersheds. Finally, the fact that using the global dataset (available for any location) for model development resulted in well-simulated streamflow and hydraulic head indicates the opportunity to apply this coupled model in data-scarce regions (lacking geological survey and aquifer property information). Nevertheless, the success of this modeling application does not guarantee the accuracy of the dataset for other locations, hence, further verification is required.

Funding

This research was funded by Research Foundation Flanders (FWO, PhD grant no. 1S11022N).

CRediT authorship contribution statement

Estifanos Addisu Yimer: Conceptualization, Methodology, Software, Validation, Formal analysis, Investigation, Writing – Original Draft, Visualization, and Funding acquisition. **Lorenzo Villani**.: Methodology, Formal analysis, Visualization, Writing- Original draft. **Ryan T. Bailey**: Software, Resources, Data Curation, Supervision. **Bert Van Schaeybroeck**: Methodology, Validation, Supervision, Writing – Original Draft. **Hans Van De Vyver**: Methodology, Validation, Supervision, Writing – Original Draft. **Jiri Nossent**: Methodology, Validation, Supervision, Writing – Original Draft and Funding acquisition.: **Ann van Griensven**: Methodology, Validation, Supervision, Writing – Original Draft and Funding acquisition.

Declaration of Competing Interest

The authors declare the following financial interests/personal relationships which may be considered as potential competing interests. Estifanos Addisu Yimer reports financial support was provided by Research Foundation Flanders (FWO, PhD grant no. 1S11022N).

Data Availability

Data will be made available on request.

Acknowledgments

We would like to thank Michel Journée and Alex Dewalque for their help in providing the gridded observational data. The gridded observational data is available for research purposes and can be requested at ui@meteo.be.

Appendix A. Supporting information

Supplementary data associated with this article can be found in the online version at doi:10.1016/j.ejrh.2023.101532.

References

Aliyari, F., Bailey, R.T., Tasdighi, A., Dozier, A., Arabi, M., Zeiler, K., 2019. Coupled SWAT-MODFLOW model for large-scale mixed agro-urban river basins. Environ. Model. Softw. 115, 200–210.

Al-Safi, H.I.J., Kazemi, H., Sarukkalige, P.R., 2020. Comparative study of conceptual versus distributed hydrologic modelling to evaluate the impact of climate change on future runoff in unregulated catchments. J. Water Clim. Change 11, 341–366.

Arnold, J.G., Srinivasan, R., Muttiah, R.S., Williams, J.R., 1998. Large area hydrologic modeling and assessment part I: model development 1. JAWRA J. Am. Water Resour. Assoc. 34, 73–89.

Avery, C., 1994. Interaction of ground water with the Rock River near Byron, Illinois. US Department of the Interior, US Geological Survey.

Bailey, R.T., Wible, T.C., Arabi, M., Records, R.M., Ditty, J., 2016. Assessing regional-scale spatio-temporal patterns of groundwater–surface water interactions using a coupled SWAT-MODFLOW model. Hydrol. Process. 30, 4420–4433.

Bailey, R.T., Bieger, K., Arnold, J.G., Bosch, D.D., 2020. A new physically-based spatially-distributed groundwater flow module for SWAT+. Hydrology 7, 75.

Bailey, R.T., Bieger, K., Flores, L., Tomer, M., 2022. Evaluating the contribution of subsurface drainage to watershed water yield using SWAT+ with groundwater modeling. Sci. Total Environ. 802, 149962.

Barthel, R., Banzhaf, S., 2016. Groundwater and surface water interaction at the regional-scale–a review with focus on regional integrated models. Water Resour. Manag. 30, 1–32.

Bastola, S., Misra, V., 2014. Evaluation of dynamically downscaled reanalysis precipitation data for hydrological application. Hydrol. Process. 28, 1989–2002.
Bauer, P., Gumbricht, T., Kinzelbach, W., 2006. A regional coupled surface water/groundwater model of the Okavango Delta, Botswana. Water Resour. Res. 42.
Bieger, K., Arnold, J.G., Rathjens, H., White, M.J., Bosch, D.D., Allen, P.M., Volk, M., Srinivasan, R., 2017. Introduction to SWAT+, a completely restructured version of the soil and water assessment tool. JAWRA J. Am. Water Resour. Assoc. 53, 115–130.
Blöschl, G., Montanari, A., 2010. Climate change impacts—throwing the dice? Hydrol. Process.: Int. J. 24, 374–381.
Brouwers, J., Peeters, B., Van Steertegem, M., van Lipzig, N., Wouters, H., Beullens, J., Demuzere, M., Willems, P., De Ridder, K., Maiheu, B., 2015. MIRA klimaatrapport 2015: over waargenomen en toekomstige klimaatveranderingen.
Choi, W., Kim, S.J., Rasmussen, P.F., Moore, A.R., 2009. Use of the North American Regional reanalysis for hydrological modelling in manitoba. Can. Water Resour. J. 34, 17–36.
Conant Jr, B., 2004. Delineating and quantifying ground water discharge zones using streambed temperatures. Groundwater 42, 243–257.
Cornes, R.C., van der Schrier, G., van den Besselaar, E.J., Jones, P.D., 2018. An ensemble version of the E-OBS temperature and precipitation data sets. J. Geophys. Res.: Atmos. 123, 9391–9409.
Coustau, M., Rousset-Regimbeau, F., Thirel, G., Habets, F., Janet, B., Martin, E., de Saint-Aubin, C., Soubeyroux, J.-M., 2015. Impact of improved meteorological forcing, profile of soil hydraulic conductivity and data assimilation on an operational Hydrological Ensemble Forecast System over France. J. Hydrol. 525, 781–792.
Dams, J., Salvadore, E., Van Daele, T., Batelaan, O., 2009. Case kleine nete: hydrologie: wetenschappelijk rapport-NARA 2009.
Deb, P., Kiem, A.S., Willgoose, G., 2019. A linked surface water-groundwater modelling approach to more realistically simulate rainfall-runoff non-stationarity in semi-arid regions. J. Hydrol. 575, 273–291.
Devito, K.J., Hill, A.R., Roulet, N., 1996. Groundwater-surface water interactions in headwater forested wetlands of the Canadian Shield. J. Hydrol. 181, 127–147.
Essou, G.R., Sabarly, F., Lucas-Picher, P., Brissette, F., Poulin, A., 2016. Can precipitation and temperature from meteorological reanalyses be used for hydrological modeling? J. Hydrometeorol. 17, 1929–1950.
Foster, S.S.D., Morris, B.L., Lawrence, A.R., 1994. Effects of urbanization on groundwater recharge, 2–3 June 1993 Groundwater Problems in Urban Areas: Proceedings of the International Conference Organized by the Institution of Civil Engineers and Held in London. Thomas Telford Publishing, pp. 43–63. https://doi.org/10.1680/gpiua.19744.0005, 2–3 June 1993.
Fryar, A.E., Wallin, E.J., Brown, D.L., 2000. Spatial and temporal variability in seepage between a contaminated aquifer and tributaries to the Ohio River. Groundw. Monit. Remediat. 20, 129–146.
Funk, C., Peterson, P., Landsfeld, M., Pedreros, D., Verdin, J., Shukla, S., Husak, G., Rowland, J., Harrison, L., Hoell, A., 2015. The climate hazards infrared precipitation with stations—a new environmental record for monitoring extremes. Sci. data 2, 1–21.
Galbiati, L., Bouraoui, F., Elorza, F.J., Bidoglio, G., 2006. Modeling diffuse pollution loading into a Mediterranean lagoon: development and application of an integrated surface–subsurface model tool. Ecol. Model. 193, 4–18.
Gassman, P.W., Reyes, M.R., Green, C.H., Arnold, J.G., 2007. The soil and water assessment tool: historical development, applications, and future research directions. Trans. ASABE 50, 1211–1250.
Guzman, J.A., Moriasi, D.N., Gowda, P.H., Steiner, J.L., Starks, P.J., Arnold, J.G., Srinivasan, R., 2015. A model integration framework for linking SWAT and MODFLOW. Environ. Model. Softw. 73, 103–116.
Habets, F., Boone, A., Champeaux, J.-L., Etchevers, P., Franchisteguy, L., Leblois, E., Ledoux, E., Le Moigne, P., Martin, E., Morel, S., 2008. The SAFRAN-ISBA-MODCOU hydrometeorological model applied over France. J. Geophys. Res.: Atmos. 113.
Harris, I., Osborn, T.J., Jones, P., Lister, D., 2020. Version 4 of the CRU TS monthly high-resolution gridded multivariate climate dataset. Sci. data 7, 1–18.
Harvey, J.W., Bencala, K.E., 1993. The effect of streambed topography on surface-subsurface water exchange in mountain catchments. Water Resour. Res. 29, 89–98.
Hayashi, M., Rosenberry, D.O., 2001. 6. Effects of groundwater exchange on the hydrology and ecology of surface waters. J. Groundw. Hydrol. 43, 327–341.
Huang, S., Kumar, R., Flörke, M., Yang, T., Hundecha, Y., Kraft, P., Gao, C., Gelfan, A., Liersch, S., Lobanova, A., 2017. Evaluation of an ensemble of regional hydrological models in 12 large-scale river basins worldwide. Clim. Change 141, 381–397.
Huscroft, J., Gleeson, T., Hartmann, J., Börker, J., 2018. Compiling and mapping global permeability of the unconsolidated and consolidated earth: global hydrogeology maps 2.0 (GLHYMPS 2.0). Geophys. Res. Lett. 45, 1897–1904. https://doi.org/10.1002/2017GL075860.
Ibrahim, B., Wisser, D., Barry, B., Fowe, T., Aduna, A., 2015. Hydrological predictions for small ungauged watersheds in the Sudanian zone of the Volta basin in West Africa. J. Hydrol.: Reg. Stud. 4, 386–397.
Jolly, I.D., McEwan, K.L., Holland, K.L., 2008. A review of groundwater–surface water interactions in arid/semi-arid wetlands and the consequences of salinity for wetland ecology. Ecohydrol.: Ecosyst., Land Water Process Interact., Ecohydrogeomorpho. 1, 43–58.
Jones, R.W., Renfrew, I.A., Orr, A., Webber, B.G.M., Holland, D.M., Lazzara, M.A., 2016. Evaluation of four global reanalysis products using in situ observations in the Amundsen Sea Embayment, Antarctica. J. Geophys. Res.: Atmos. 121, 6240–6257.
Keery, J., Binley, A., Crook, N., Smith, J.W., 2007. Temporal and spatial variability of groundwater–surface water fluxes: Development and application of an analytical method using temperature time series. J. Hydrol. 336, 1–16.
Kim, N.W., Chung, I.M., Won, Y.S., Arnold, J.G., 2008. Development and application of the integrated SWAT–MODFLOW model. J. Hydrol. 356, 1–16.
Lamontagne, S., Leaney, F.W., Herczeg, A.L., 2005. Groundwater–surface water interactions in a large semi-arid floodplain: implications for salinity management. Hydrol. Process.: Int. J. 19, 3063–3080.
Ludwig, J.A., Wilcox, B.P., Breshears, D.D., Tongway, D.J., Imeson, A.C., 2005. Vegetation patches and runoff–erosion as interacting ecohydrological processes in semiarid landscapes. Ecology 86, 288–297.
Luo, Y., Sophocleous, M., 2011. Two-way coupling of unsaturated-saturated flow by integrating the SWAT and MODFLOW models with application in an irrigation district in arid region of West China. J. Arid Land 3, 164–173.
Martina, M.L.V., Todini, E., Liu, Z., 2011. Preserving the dominant physical processes in a lumped hydrological model. J. Hydrol. 399, 121–131.
Menking, K.M., Syed, K.H., Anderson, R.Y., Shafike, N.G., Arnold, J.G., 2003. Model estimates of runoff in the closed, semiarid Estancia basin, central New Mexico, USA. Hydrol. Sci. J. 48, 953–970.
Minnig, M., Moeck, C., Radny, D., Schirmer, M., 2018. Impact of urbanization on groundwater recharge rates in Dübendorf, Switzerland. J. Hydrol. 563, 1135–1146. https://doi.org/10.1016/j.jhydrol.2017.09.058.
Moriasi, D.N., Gitau, M.W., Pai, N., Daggupati, P., 2015. Hydrologic and water quality models: performance measures and evaluation criteria. Trans. ASABE 58, 1763–1785.
Nash, J.E., Sutcliffe, J.V., 1970. River flow forecasting through conceptual models part I—A discussion of principles. J. Hydrol. 10, 282–290. https://doi.org/10.1016/0022-1694(70)90255-6.
Neitsch, S.L., Arnold, J.G., Kiniry, J.R., Williams, J.R., 2011. Soil and water assessment tool theoretical documentation version 2009. Texas Water Resources Institute.
Nguyen, T.T., Keupers, I., Willems, P., 2018. Conceptual river water quality model with flexible model structure. Environ. Model. Softw. 104, 102–117.
Nyquist, J.E., Freyer, P.A., Toran, L., 2008. Stream bottom resistivity tomography to map ground water discharge. Groundwater 46, 561–569.
Pechlivanidis, I.G., Jackson, B.M., Mcintyre, N.R., Wheater, H.S., 2011. Catchment scale hydrological modelling: a review of model types, calibration approaches and uncertainty analysis methods in the context of recent developments in technology and applications. Glob. NEST J. 13, 193–214.
Pellicer-Martínez, F., González-Soto, I., Martínez-Paz, J.M., 2015. Analysis of incorporating groundwater exchanges in hydrological models. Hydrol. Process. 29, 4361–4366.
Peterson, J.R., Hamlett, J.M., 1998. Hydrologic calibration of the swat model in a watershed containing fragipan soils 1. JAWRA J. Am. Water Resour. Assoc. 34, 531–544.
Piani, C., Weedon, G.P., Best, M., Gomes, S.M., Viterbo, P., Hagemann, S., Haerter, J.O., 2010. Statistical bias correction of global simulated daily precipitation and temperature for the application of hydrological models. J. Hydrol. 395, 199–215.

Quintana-Segui, P., Le Moigne, P., Durand, Y., Martin, E., Habets, F., Baillon, M., Canellas, C., Franchisteguy, L., Morel, S., 2008. Analysis of near-surface atmospheric variables: Validation of the SAFRAN analysis over France. J. Appl. Meteorol. Climatol. 47, 92–107.
Raimonet, M., Oudin, L., Thieu, V., Silvestre, M., Vautard, R., Rabouille, C., Le Moigne, P., 2017. Evaluation of gridded meteorological datasets for hydrological modeling. J. Hydrometeorol. 18, 3027–3041.
Shangguan, W., Hengl, T., de Jesus, J.M., Yuan, H., Dai, Y., 2017. Mapping the global depth to bedrock for land surface modeling. J. Adv. Model. Earth Syst. 9, 65–88.
Siad, S.M., Iacobellis, V., Zdruli, P., Gioia, A., Stavi, I., Hoogenboom, G., 2019. A review of coupled hydrologic and crop growth models. Agric. Water Manag. 224, 105746.
Silliman, S.E., Booth, D.F., 1993. Analysis of time-series measurements of sediment temperature for identification of gaining vs. losing portions of Juday Creek, Indiana. J. Hydrol. 146, 131–148.
Sophocleous, M.A., Koelliker, J.K., Govindaraju, R.S., Birdie, T., Ramireddygari, S.R., Perkins, S.P., 1999. Integrated numerical modeling for basin-wide water management: the case of the Rattlesnake Creek basin in south-central Kansas. J. Hydrol. 214, 179–196.
Spruill, C.A., Workman, S.R., Taraba, J.L., 2000. Simulation of daily and monthly stream discharge from small watersheds using the SWAT model. Trans. ASAE 43, 1431.
Sreedevi, S., Kunnath-Poovakka, A., Eldho, T.I., 2021. Comparison of Conceptual and Distributed Hydrological Models for Runoff Estimation in a River Basin. In: The Ganga River Basin: A Hydrometeorological Approach. Springer, pp. 135–148.
Sridhar, V., Billah, M.M., Hildreth, J.W., 2018. Coupled surface and groundwater hydrological modeling in a changing climate. Groundwater 56, 618–635.
Srivastava, P., McNair, J.N., Johnson, T.E., 2006. Comparison of process-based and artificial neural network approaches for streamflow modeling in an agricultural watershed 1. JAWRA J. Am. Water Resour. Assoc. 42, 545–563.
Sun, W., Ishidaira, H., Bastola, S., Yu, J., 2015. Estimating daily time series of streamflow using hydrological model calibrated based on satellite observations of river water surface width: Toward real world applications. Environ. Res. 139, 36–45.
Tam, V.T., Nga, T.T.V., 2018. Assessment of urbanization impact on groundwater resources in Hanoi, Vietnam. J. Environ. Manag. 227, 107–116.
Tarek, M., Brissette, F., Arsenault, R., 2021. Uncertainty of gridded precipitation and temperature reference datasets in climate change impact studies. Hydrol. Earth Syst. Sci. 25, 3331–3350.
Van Camp, M., Coetsiers, M., Martens, K., Walraevens, K., 2010. Effects of multi-annual climate variability on the hydrodynamic evolution (1833 to present) in a shallow aquifer system in northern Belgium. Hydrol. Sci. J. 55, 763–779.
Van der Kamp, G., Hayashi, M., 2009. Groundwater-wetland ecosystem interaction in the semiarid glaciated plains of North America. Hydrogeol. J. 17, 203.
Vu, M.T., Raghavan, S.V., Liong, S.-Y., 2012. SWAT use of gridded observations for simulating runoff–a Vietnam river basin study. Hydrol. Earth Syst. Sci. 16, 2801–2811.
Waibel, M.S., Gannett, M.W., Chang, H., Hulbe, C.L., 2013. Spatial variability of the response to climate change in regional groundwater systems–examples from simulations in the Deschutes Basin, Oregon. J. Hydrol. 486, 187–201.
Wang, Y., Chen, N., 2021. Recent progress in coupled surface–ground water models and their potential in watershed hydro-biogeochemical studies: a review. Watershed Ecol. Environ. 3, 17–29.
Woo, M.-K., Thorne, R., 2006. Snowmelt contribution to discharge from a large mountainous catchment in subarctic Canada. Hydrol. Process.: Int. J. 20, 2129–2139.
Wossenyeleh, B.K., Worku, K.A., Verbeiren, B., Huysmans, M., 2021. Drought propagation and its impact on groundwater hydrology of wetlands: a case study on the Doode Bemde nature reserve (Belgium). Nat. Hazards Earth Syst. Sci. 21, 39–51.
Yatagai, A., Arakawa, O., Kamiguchi, K., Kawamoto, H., Nodzu, M.I., Hamada, A., 2009. A 44-year daily gridded precipitation dataset for Asia based on a dense network of rain gauges. Sola 5, 137–140.
Yimer, E.A., Van Schaeybroeck, B., Van de Vyver, H., Van Griensven, A., 2022. Evaluating probability distribution functions for the standardized precipitation evapotranspiration index over Ethiopia. Atmosphere 13, 364. https://doi.org/10.3390/atmos13030364.
Yimer, E.A., T. Bailey, T.B., Leda Piepers, L., Nossent, J., Van Griensven, A., 2023. Improved Representation of Groundwater–Surface Water Interactions Using SWAT +gwflow and Modifications to the gwflow Module. Water 15. https://doi.org/10.3390/w15183249.
Yimer, E.A., Riakhi, F.-E., Bailey, R.T., Nossent, J., van Griensven, A., 2023a. The impact of extensive agricultural water drainage on the hydrology of the Kleine Nete watershed, Belgium. Sci. Total Environ., 163903 https://doi.org/10.1016/j.scitotenv.2023.163903.
Yimer, E.A., Yadollahi, S., Riakhi, F.-E., Alitane, A., Weerasinghe, I., Wirion, C., Nossent, J., van Griensven, A., 2023b. A groundwater level-based filtering to improve the accuracy of locating agricultural tile drain and ditch networks. Int. J. Appl. Earth Obs. Geoinf. 122, 103423.
You, Q., Min, J., Zhang, W., Pepin, N., Kang, S., 2015. Comparison of multiple datasets with gridded precipitation observations over the Tibetan Plateau. Clim. Dyn. 45, 791–806.
Zomlot, Z., Verbeiren, B., Huysmans, M., Batelaan, O., 2015. Spatial distribution of groundwater recharge and base flow: Assessment of controlling factors. J. Hydrol.: Reg. Stud. 4, 349–368. https://doi.org/10.1016/j.ejrh.2015.07.005.